Energy, Exergy, Environmental Impact and Economic (4E) Analysis of ET-CPC-Powered Solar Domestic Water Heating System

Dinesh K Sharma (dinesh.sharma@skit.ac.in)
Swami Keshvanand Institute of Technology Management and Gramothan https://orcid.org/0000-0003-3919-1900

Dilip Sharma
Malaviya National Institute of Technology Department of Mechanical Engineering

Ahmed Hamza H. Ali
Assiut University Faculty of Engineering

Research Article

Keywords: Energy, Exergy, Environmental impact, Economic, evacuated tube, compound parabolic concentrator

Posted Date: January 17th, 2022

DOI: https://doi.org/10.21203/rs.3.rs-1150649/v1

Energy, Exergy, Environmental Impact and Economic (4E) Analysis of ET-CPC-powered Solar Domestic Water Heating System

Author1 (Corresponding Author)

Dinesh Kumar Sharma

[1]Department of Mechanical Engineering,
Swami Keshavanand Institute of Technology, Management and Gramothan, Jaipur-302017, India

[2]Department of Mechanical Engineering,
Malaviya National Institute of Technology, Jaipur-302017, India

Email: dinesh.sharma@skit.ac.in

Author 2

Dilip Sharma

[2]Department of Mechanical Engineering,
Malaviya National Institute of Technology, Jaipur-302017, India

Email: sharmadmnit@gmail.com

Author 3

Ahmed Hamza H. Ali[3]

[3]Department of Mechanical Engineering, Assiut University, Assiut-71516, Egypt

Email: drahmedhamza@yahoo.com, ah-hamza@aun.edu.eg

Energy, Exergy, Environmental Impact and Economic (4E) Analysis of ET-CPC-powered Solar Domestic Water Heating System

Dinesh Kumar Sharma[1,2*], Dilip Sharma[2], Ahmed Hamza H. Ali[3]

[1]Department of Mechanical Engineering, Swami Keshavanand Institute of Technology, Management and Gramothan, Jaipur-302017, India

[2]Department of Mechanical Engineering, Malaviya National Institute of Technology, Jaipur-302017, India

[3]Department of Mechanical Engineering, Faculty of Engineering, Assiut University, Assiut-71516, Egypt

*Corresponding Author: dinesh.sharma@skit.ac.in

Abstract

World energy demand is increasing continuously; consequently, the environmental impact forces towards utilizing renewable energy resources with efficient and optimized cost-performance conversion technologies. Therefore in this study, an analytical model is developed to propose the energy, exergy, environmental impact and economic (4E) analysis of the water heating system at Jaipur (India) with evacuated tube compound parabolic concentrator ET-CPC field of the total area of 81m^2. The model results were validated with the experimental data, and a good agreement has prevailed. After that, the model is used to perform parametric studies on the effect of operating and meteorological parameters on the productivity and performance of the system. Moreover, the system's performance, environmental impact and economic aspects have been investigated and compared under different meteorological conditions at four different locations in Rajasthan (India) using TMY2 weather data files. Results clarified that Jodhpur receives the highest solar radiation intensity from these four locations. Consequently, the results indicate the highest annual energy and exergy with the value of 79.72 MWh and 9.311 MWh followed by Jaisalmer, Barmer, and Jaipur. The economic analysis results clarified that the simple payback

period ranged from 4.5 to 4.75 years and the discounted payback period ranged from 6.6 to 7 years based on a 6% discount rate. At the same time, the Levelized Cost of Heating (LCOH) ranges from 1.62 to 1.72 INR/kWh of heat compared to closest with CNG as fuel ranging from 4.39 to 4.41 INR/kWh for specified locations. The internal rate of return is reported to be 16.76, 16.82, 16.77, and 16.75% for Barmer, Jodhpur, Jaipur, and Jaisalmer respectively, and savings of 74400, 78125, 75371, and 73813 kg of CO_2 emission to the environment.

Keywords

Energy; Exergy; Environmental impact; Economic; evacuated tube; compound parabolic concentrator.

Nomenclature

CC	construction cost
CF	cash inflows
CPC	compound parabolic concentrator
DPBP	discounted payback period
ETC	evacuated tube collector
ET-CPC	evacuated tube with compound parabolic concentrator
FPC	flat plate collector
IRR	internal rate of return
LCOH	Levelized Cost of Heating
PCM	phase change material
PTC	parabolic trough collector
RTD	resistance temperature detector
SDWH	solar domestic water heating
SPBP	simple payback period
SPV	solar photo-voltaic
STC	solar thermal collector
TES	thermal energy storage
TLCC	total life cycle cost

Symbols and notations

A	area (m^2)
C_f	specific heat (J/kg.K)
D	tube diameter (m)
dt	time difference (s)
Ex	exergy (W/m^2)
f	friction factor
F_R	heat removal factor
I_T	total solar radiation (W/m2)
L	length (m)
$\dot{m}_f$	mass flow rate (kg/s)

P	pressure (kPa)
Q_{useful}	useful heat gain (kWh)
V	fluid velocity (m/s)
U_L	overall heat coefficient ($W/m^2.K$)

Greek letter

α	absorptivity
ρ	density
η	efficiency
μ	kinematic viscosity
τ	transmissivity

Subscript

amb	ambient
c	collector
f	fluid
in	inlet
m	mean
n	number of collector in-series
out	outlet
r	receiver

1. Introduction

Once a luxury afforded to a precious few, energy has become a commodity that the modern world cannot survive without (Shekarchian et al. 2013). Most of the day-to-day needs of modern society are rigorously increasing the energy demand whether it refers to cooling, heating, or power. Presently, conventional sources dominate to produce electricity and are responsible for contributing harmful pollutants to the environment. Renewable energy such as solar energy has been proven to meet the energy demand partially or fully without carbon footprints being a clean fuel. Solar thermal collectors (STCs) and solar photo-voltaic panels (SPVs) are widely accepted for harnessing solar energy and further utilizing it for cooling, heating, and power. Flat plate collectors (FPCs), compound parabolic concentrator (CPC), evacuated tube collectors (ETCs), parabolic trough collectors (PTCs), etc. are some of the popular STC technologies. Recent innovations and technology advancements such as evacuated tube integrated with CPC (termed as ET-CPC), evacuated tube integrated with PTC, and many others are with improved productivity and efficiency by lowering losses to the environment which resulted in achieving higher

97 working temperature. Out of these, ET-CPCs are the most preferred for medium operational temperature
98 range (up to 150°C) applications being a stationary type of STC. At the same time, these offer better
99 productivity utilizing diffusive and direct radiations with efficiency ranging from 35 to 55%.

100 Domestic/community water heating is an essential application that is relatively energy-intensive, and the
101 use of conventional resources such as kerosene, natural gas, wood, coal, and electricity is quite expensive
102 and emits harmful emissions. Formerly, FPCs have been primarily promoted but as time progressed,
103 technology advancement in STCs took place as discussed above. Sokhansefat et al. (2018) compared the
104 FPC and ETC solar collectors in cold climatic conditions based on thermoeconomic and environmental
105 impact analysis. It was reported that the performance of the ETC system is 41% better than the FPC
106 system, and the yearly practical heat gain of ETC is 30% more than that of FPC in any climate zone.
107 Hazami et al. (2013) reported a year-round energy performance monitoring results of a new type of
108 domestic solar water heating system (DSWH) based on ETC. It was also reported that ETC generated
109 about 9% more energy than the FPC under the same climatic condition. Kabeel et al. (2020) reported
110 improved thermal performance of modified ETC with the help of hybrid storage materials and low-cost
111 concentrators. Thermal efficiency improvement of modified design for using hybrid storage materials
112 reached 72.1%. They used 0.0, 2, 3, 4, and 5% graphite nanomaterial mass concentration as hybrid
113 storage materials.

114 Geete et al. (2019) fabricated compound parabolic solar collectors with evacuated tubes and analyzed the
115 thermal performance of the system. Instantaneous energy efficiency was reported to be 69.87% during
116 their experimental work. Jiang et al. (2015) concluded from their studies that CPC integrated ETCs (ET-
117 CPCs) showed 50% efficiency at 200°C using mineral oils. Ma et al. (2010) reported that improving
118 thermal conductance of working fluid from 5 to 40 W/m.K using ET-CPCs helped increase the efficiency
119 by 10% and outlet temperature by 16%. Hence, the use of CPC reflectors at the backside of the ETC tubes
120 is helpful to increase the collector efficiency by improving the overall aperture area. Similarly, Pie et al.
121 (2012) analyzed the evacuated tube CPC and concluded that the concentrator is helpful to improve the

thermal performance of the ETC in high-temperature ranges. Further, Mills et al. (1986) reported a study on the effect of the acceptance angle of CPC on the performance of the evacuated tubes. They concluded that the acceptance angle is less decisive but the aperture area. Performance of ET-CPC is reported to have negligible effect from the selection of orientations from either North-South or East-West. The selection of reflector material was also discussed and suggested that the use of polished stainless steel is better in terms of cost-effectiveness, durability, and maintenance compared to other mirror materials.

Previously, Mishra et al. (2017) compared the performance of ETC and ET-CPC based on energy and exergy analyses. It was reported that 27.28% extra gain was observed in energy by using evacuated tube CPC compared to that of without CPC. Kerme et al. (2017) presented energy and exergy analysis of solar-powered vapor absorption systems. Furthermore, the result also indicated that the main source of the exergy destruction is the solar collector. In the solar collector, 71.9% of the input exergy was destroyed which accounted for 84% of the total exergy loss. Chopra et al. (2021) reported a 4E analysis of a PCM (palmatic acid) embedded ETC-powered solar water heating system. A significant improvement was shown in energy, exergy, and CO_2 mitigation with the use of ETC with PCM compared to without PCM. The results claimed a rise of 36-44% in energy efficiency whereas a rise of 28-35% was observed in exergy efficiency with the use PCM filled in annular space between absorber and tube of ETC.

Battisti and Corrado (2005) applied environmental analysis and optimization to the water storage coupled solar thermal collector. Simapro software program was used to obtain environmental indicators. It was found that the reduction of the impacts could be up to 40% and the environmental payback times were 5–19 months. Faizal et al. (2015) applied the energy, exergy, economic, and environmental analysis on a flat-plate solar collector operated with SiO_2 nanofluid. It was found that the energy and exergy efficiencies of nanofluids were higher than base fluids. Also, CO_2 emissions and payback periods of nanofluids are better. Bellos et al. (2017) reported a 4E analysis for a solar-assisted refrigeration system for various operating scenarios. Evacuated tube collectors fed heat to the generator of the vapour

absorption chiller. The electricity savings were 53.98%, the IRR 6.6%, and the payback period close to 14 years.

Thus, it can be concluded that ET-CPCs are quite efficient at elevated temperatures up to 200°C and have no need for a solar tracking mechanism, which makes them a preferred choice over FPC. Along with this, these utilize diffuse and direct types of solar radiation. The thermodynamic performance of ET-CPCs based solar water heating systems has been measured through energy and exergy analyses. Energy analysis is conservative as per the first law of thermodynamics which typically involves energy efficiency and gain. On the other hand, exergy analysis helps to determine the energy transactions based on quality. Exergy analysis denotes the maximum theoretical work that can be obtained in a given set of environmental conditions. Hence, a thermodynamic system can be better assessed with the help of an exergy method (Caliskan 2017). Also, exergy analysis helps to determine the sustainability of the system (Moran and Shapiro 1993). An overall analysis of the system is incomplete without understanding its monetary transactions and environmental impact during its entire useful life (Dincer and Rosen 2007a)(Meyer et al. 2009)(Tsatsaronis and Morosuk 2012). The first law of thermodynamics is widely used for energy utilization analysis. However, it is limited because it is incapable of quantitatively determining the quality of energy. On the other hand, the second law of thermodynamics supplants this limitation by introducing the exergy analysis that quantifies the potential helpful work for a given amount of energy. Therefore, it is essential that both the quantity and quality of the energy used for practical energy usage be considered (Saidur et al. 2013)(Cengel and Boles 2019). Expressing the true efficiency makes the exergy a powerful tool in sectoral energy analysis and engineering design (Rosen and Dincer 1997). It should be pointed out that economic analysis is indirectly affected by environmental impact and energy analysis results.

In the present work, an analytical model is developed to carry out energy, exergy, environmental impact and economic analysis of an 81 m^2 ET-CPC powered solar water heating system equipped with thermal energy storage. Along with this, a parametric study is also performed to report the effect of mass flow

rate, solar radiation intensity, and ambient temperature on productivity and efficiency of reported installation at various fluid inlet temperatures. It was identified that overall analysis of ET-CPC-based applications are less reported in the literature and thus sufficient data is not available which can be otherwise helpful to promote its use. Thus, the thermodynamic performance of the SDWH system with its environmental impact and economic aspects has been investigated and compared under meteorological conditions of four different locations of Rajasthan (India) using TMY2 weather data files.

2. System Description and Methodology

The system presented in this research is installed at the roof and front lawn of the Department of Mechanical Engineering, Malaviya National Institute of Technology, Jaipur (26.86° N, 75.81° E). The schematic and actual photograph is presented in Figure 1. Each ET-CPC module has an effective area of 3 m^2. As shown in Figure 1, the installed ET-CPC field is arranged as six rows having four ET-CPCs in series, and one row has three ET-CPCs in-series constituting a total aperture area of 81 m^2 with 27 ET-CPC modules. These ET-CPCs are connected with a sensible thermal energy storage tank (containing soft water as a working medium) with the help of a centrifugal pump. Figure 2 shows the pictorial view of the ET-CPC solar field. The technical descriptions of the ET-CPC, thermal energy storage tank, and pump are provided in Table 1. There is no load considered to this system in the specified time. Various thermocouples, RTDs, and flow meters have been installed as shown in Figure 1 and a 16 channel Masibus 85xx+ data logger has been used to integrate these data.

This study developed an analytical model for energy, exergy, environmental impact and economic analysis of this SDWH. Further, experimental validation of the model is carried out using energetic efficiency and useful heat gain from the system. A parametric study is also made to investigate the effect of the mass flow rate of working fluid, solar radiation intensity, and ambient temperature on the productivity and efficiency of the system. Four potential locations have been identified from Rajasthan (India); Barmer, Jodhpur, Jaisalmer, and Jaipur. Weather data have been taken from the TMY2 file of these identified locations for ambient temperature and solar radiation intensity around the year. Energy

and exergy gain along with energy efficiency and exergetic efficiency is then estimated and compared for the specified locations. As discussed earlier, no analysis could be decisive without environmental and economic evaluation. Hence, environmental analysis is carried out to show the amount of CO_2 emissions saved. In the latter section, economic analysis is done while comparing SDWH with the conventional methods of water heating.

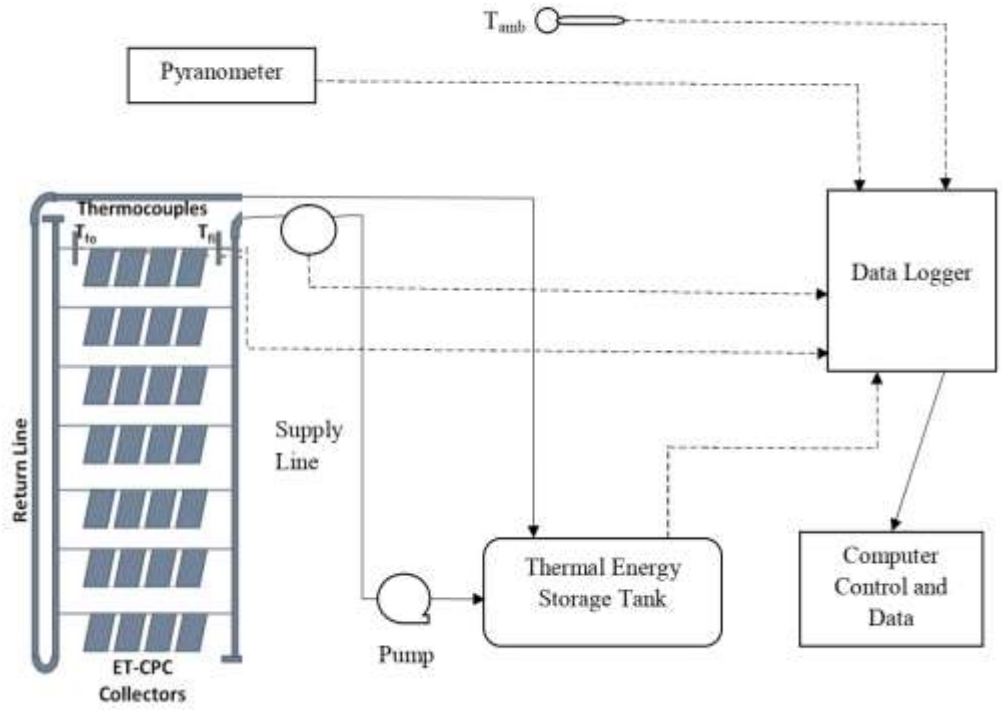

Figure 1 Schematic diagram of ET-CPC solar domestic water heating system

Figure 2 Pictorial view of ET-CPC solar collector field installed on MNIT, Jaipur roof top

Table 1 Technical description of the various components in the system

Description	Unit	Technical Specification
Solar Collectors		
No. of evacuated tubes	nos.	18
η_0 concerning aperture,EN12975	%	64.2
Heat transfer Coefficient (a_1)	(W/m^2K)	0.89
Temperature dependent transfer Coefficient (a_2)	(W/m^2K^2)	0.001
Grid dimensions	m	2.08 x 1.64 x 0.10
Aperture area	m^2	3.41
Max Working overpressure	bar	10
Max Stagnation temperature	^oC	250
Glass Tube Material		Borosilicate Glass 3.3
Selective Absorber coating material		Aluminum Nitride
Glass Tube (Φ Ext/ Φ Int/ Wall Thickness/Tube length)	mm	47/37/1.6/1500
Make		Linuo-Ritter
Hot Storage Tank		
Tank Diameter	m	1
Tank Length	m	3.5
Volume of Tank	m^3	2.2
Material of Tank		Mild Steel
Insulation Material		Fiberglass of 50 mm thickness cladded with aluminium sheet
Orientation of Tank		Horizontal
Hot Water Pump		
Hot Water Pump at 25 m head	m^3/hr	5.4

Table 2 Design parameters of ET-CPC field

Parameter	Value
R	0.0185 m
C_f	4186 J/kg.K
L	1500 mm
A_r	0.1734 m^2
A	0.2215 m^2
$A_{c,total}$	81 m^2
n	12
τ	0.95

α	0.80
ρ_f	997 kg/m^3
$\dot{m}_f$	0.0357 (kg/s)
U_{tpa}	2.1 W/m^2.K
h_{pf}	100 W/m^2.K
F'	0.986

3. Energy, Exergy, Environment impact and Economic Analysis

3.1 Energy analysis of ET-CPC

Energy analysis for ET-CPC first involves the rise in fluid inlet temperature upon exit point from the ET-CPC arrays. This temperature gain is achieved from the equations developed by Mishra et al. (2017). It's essential to understand the flow distribution inside an ET-CPC module so that assessment of flow rate inside a tube could be done perfectly. Figure 3 shows the flow scattering inside a single module of ET-CPC which supports the precise number of evacuated tubes linked in series in the current setup.

Table 3 Energy Analysis of ET-CPC

Energy Analysis of ET-CPC	**Eq. No.**
$T_{out,n}$ outlet temperature from the nth ET-CPCs coupled in series is deliberate as in (Mishra et al. 2015): $$T_{out,n} = \frac{(A_c F_R \alpha\tau)_1}{\dot{m}_f C_f} \times \frac{(1-K_{eff})^n}{(1-K_{eff})} I_T + \frac{(A_r F_R U_L)_1}{\dot{m}_f C_f} \times \frac{(1-K_{eff})^n}{(1-K_{eff})} T_{amb} + K_{eff}^n T_{in}$$ Where, $$K_{eff} = 1 - \frac{A_r F_R U_{L:}}{\dot{m}_f C_f}$$ $$F_R = \frac{\dot{m}_f C_f}{U_L A_r}\left[1 - \exp\left(-\frac{2\pi r L U_L}{\dot{m}_f C_f}\right)\right]$$	1
Practical heat gain for the n-tube connected in series is given as: $$Q_{useful,n} = (\alpha\tau)_{eff} I_T - (UA)_{eff}(T_{in} - T_{amb})$$	2

Where,

$$(\alpha\tau)_{eff} = A_c F_R \alpha\tau \left(\frac{1-K_{eff}^n}{1-K_{eff}} \right)$$

$$(UA)_{eff} = A_r F_R U_L \left(\frac{1-K_{eff}^n}{1-K_{eff}} \right)$$

Instantaneous thermal efficiency ($\eta_{Instantaneous}$) is given as

$$\eta_{Instantaneous} = \frac{Q_{useful}}{\eta_{opt} \times A_{c,total} \times I_T}$$

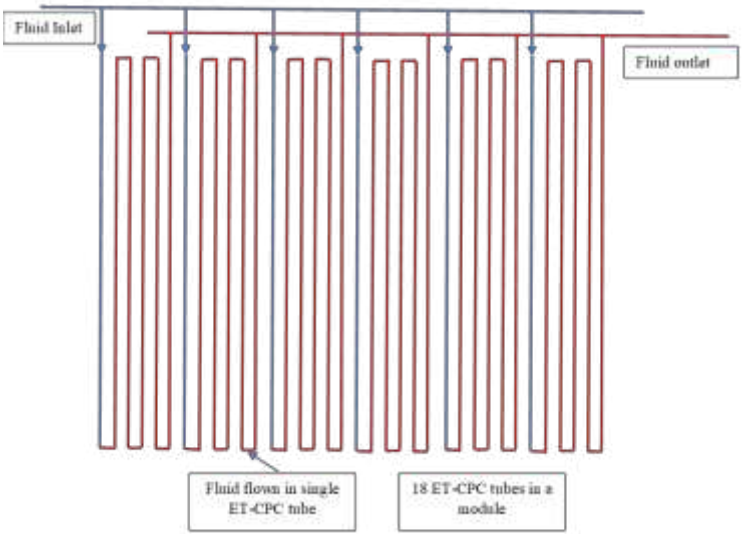

Figure 3 Fluid Flow Diagram inside an ET-CPC module

Table 3 describes reduced equations for desired energy analysis of ET-CPC solar field. In the existing setup, each ET-CPC module involves 18 evacuated tubes and four modules linked in series to create an array and equally 7 rows are arranged parallel. Hence, 12 tubes are linked in series and hence mass flow rate is distributed in 7 rows and 6 subdivisions. Hence, a total mass flow rate is 0.83 kg/s out of centrifugal pump rated discharge 1.5 kg/s because of pressure drop

due to ET-CPC solar collectors but only 0.0198 kg/s mass flow rate is observed inside any particular evacuated tube for this setup as shown in Figure 3.

Since this system's thermal energy storage is 2.2 m^3 in volume and oriented horizontally, a complete energy mix model is considered inside the TES tank. Further, energy gain is calculated as the successive sum of the energy gains, and subsequent temperature rise at any given time is treated as per equation (3) of Table 3.

3.2 Exergy analysis of ET-CPC

As stated in the Introduction section, reported literature mainly considers the physical conditions for exergy analysis and further for exergy gain. These models did not reflect the actual in-sight on the exergy destructions in each phase. Thus presented model is prepared concerning various possible destructions while performing exergy analysis therefore, accurate results could be presented. Figure 4 reports the various exergy destructions from an ET-CPC tube, and table 4 shows the various equations reduced for exergy analysis.

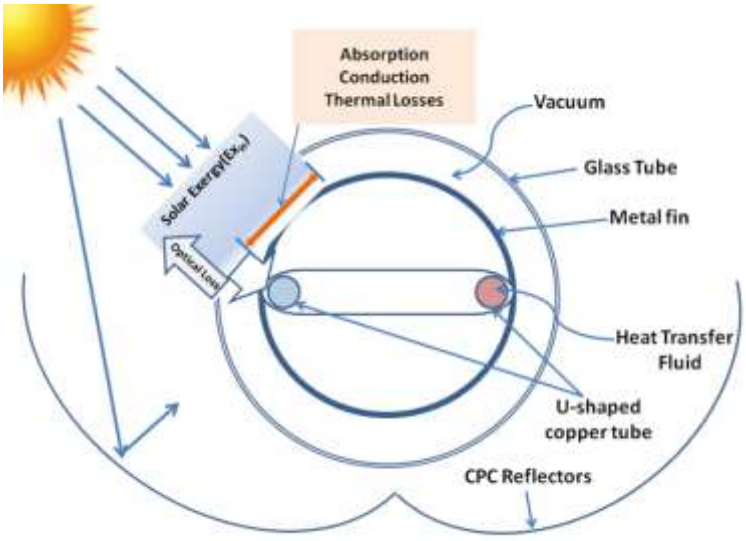

Figure 4 Representation of various Exergy Destructions inside a single ET-CPC

Table 4 Exergy Analysis of ET-CPC

Exergy Analysis of ET-CPC	**Eq. No.**
Exergy balance equation in the steady-state condition	
$\dot{E}x_{in} = \Delta\dot{E}x_{opt} + \Delta\dot{E}x_{abs} + \Delta\dot{E}x_{thermal} + \Delta\dot{E}x_{cond} + \Delta\dot{E}x_{friction} + \dot{E}x_{useful}$	4
Exergy inlet (Petela 2003, 2005)	
$\dot{E}x_{Sun} = \dot{E}x_{in} = A_{c,total} I_T \, \varphi_{solar\,rad,\max}$ $\varphi_{Solarrad,\max} = \left[1 + \frac{1}{3}\left(\frac{T_{amb}}{T_{sun}} \right)^4 - \frac{4}{3}\left(\frac{T_{amb}}{T_{sun}} \right) \right]$	5
Exergy destruction due to optical	
$\Delta\dot{E}x_{opt} = \dot{E}x_{sun}(1 - \eta_{opt})$	6
Exergy destruction due to absorption	
$\Delta\dot{E}x_{abs} = \eta_{opt}\left(\dot{E}x_{sun} - I_T \times A_{c,total}\left(1 - \frac{T_{amb}}{T_{receiver}} \right) \right)$	7
Exergy destruction due to thermal losses	
$\Delta\dot{E}x_{thermal} = K_{loss}\left(T_{surface} - T_{amb} \right)\left(1 - \frac{T_{amb}}{T_{surface}} \right)$	8
Exergy destruction due to conduction	
$\Delta\dot{E}x_{cond} = T_{amb}(\Delta S_{cond})$ $\Delta S_{cond} = \int_{Tin}^{Tout} \frac{\dot{m}_f C_f dT}{T} - \frac{1}{T_{receiver}} \int_{Tin}^{Tout} \dot{m}_f C_f dT$ $\Delta S_{cond} = \dot{m}_f C_f \left[\ln\left(\frac{T_{out}}{T_{in}} \right) - \left(\frac{T_{out} - T_{in}}{T_{receiver}} \right) \right]$	9
Exergy destruction due to pipe friction (Bejan et al. 1981)	
$\Delta\dot{E}x_{friction} = \frac{\dot{m}_f T_{amb} \Delta P}{\rho_f T_{in}}$ $\Delta P = f \, \rho_f \, L \frac{V^2}{2D}$	10

$$f = \frac{64}{\mathrm{Re}}, \text{ for } \mathrm{Re} \leq 2200$$

$$f = 0.316\,\mathrm{Re}^{-0.25}, \text{ for } \mathrm{Re} > 2200$$

$$\mathrm{Re} = \frac{\rho_f V D}{\mu_f}$$

Exergy useful

$$\dot{E}x_{useful} = \dot{E}x_{in} - (\Delta\dot{E}x_{opt} + \Delta\dot{E}x_{abs} + \Delta\dot{E}x_{thermal} + \Delta\dot{E}x_{cond} + \Delta\dot{E}x_{friction}) \quad (11)$$

Total Exergy gain

$$Ex_{gain,total} = \int \dot{E}x_{useful}.A_{total}.dt \quad (12)$$

Exergetic efficiency

$$\psi_{exergetic} = \frac{\dot{E}x_{useful}}{\dot{E}x_{in}} \quad (13)$$

3.3 Thermodynamic Analysis of Thermal Energy Storage

Thermodynamic analysis of thermal energy storage has been performed under actual environmental conditions during the charging, storing, and discharging phase. Equations for energy and exergy parameters have been reduced as presented in Table 5, and these are analyzed in conjunction with the performance of ET-CPC.

Table 5 Thermodynamic Analysis of Thermal Energy Storage

Thermodynamic Analysis of Thermal Energy Storage	Eq. No.
TES charging stage (Rezaie et al. 2015)	
Energy Balance (Dincer and Rosen 2007)(Rosen and Dincer 2003)	
$Q_{in,TES} - Q_{loss,TES} = \Delta U_{charging}$	
$\Delta U_{charging} = m_{total} C_f \Delta T_m$	
$m_{charging} = \frac{Q_{in,TES}}{C_f (T_{c,in} - T_{c,out})}$	14

Energy Efficiency

$$\eta_{charging} = \frac{Energy\,accumulated\,in\,TES}{Energy\,Input} = \frac{\Delta U_{charging}}{Q_{in,TES}} \quad (15)$$

Exergy Balance

$$Ex_{c,in} = m_{charging}\left[\left(h_{c,in} - h_{c,out}\right) - T_{amb}\left(s_{c,in} - s_{c,out}\right)\right]$$

$$Ex_{c,loss} = Q_{loss,TES}\left(1 - \frac{T_{amb}}{T_m}\right)$$

$$Ex_{c,accum} = Ex_{c,f} - Ex_{c,i} = m_{total}\left[\left(u_{c,f} - u_{c,i}\right) - \left(s_{c,f} - s_{c,i}\right)\right] \quad (16)$$

Exergy Destruction

$$\Delta Ex_{charging} = Ex_{c,in} - Ex_{c,loss} - Ex_{c,accum} \quad (17)$$

Exergy Efficiency

$$\psi_{charging} = \frac{Exergy\,accumulated\,in\,TES}{Exergy\,Input} = \frac{Ex_{c,accum}}{Ex_{c,in}} \quad (18)$$

TES Storing Stage

Energy Efficiency

$$\eta_{storing} = \frac{Energy\,Accumulation\ in\ TES\,during\,charging\,and\,storing}{Energy\,Accumulation\ in\ TES\,during\,charging} \quad (19)$$

Exergetic Efficiency

$$\psi_{storing} = \frac{Exergy\,Accumulation\ in\ TES\,during\,charging\,and\,storing}{Exergy\,Accumulation\ in\ TES\,during\,charging} \quad (20)$$

TES Discharging Stage

Energy recovered

$$Q_{rec} = -\left(\Delta U_{discharge} + Q_{loss,TES}\right)$$

$$\Delta U_{discharge} = m_{total} C_f \Delta T_m$$

$$m_{discharging} = \frac{Q_{rec}}{C_f\left(T_{d,out} - T_{d,in}\right)} \quad (21)$$

Energy Efficiency

$$\eta_{discharging} = \frac{Energy\,recovered\,by\,TES}{Energy\,released\,by\,TES} = \frac{Q_{rec}}{Q_{rec} + Q_{loss,TES}} \quad (22)$$

Exergy recovered

$$Ex_{rec} = m_{discharge}\left[\left(h_{d,out} - h_{d,in}\right) - T_{amb}\left(s_{d,out} - s_{d,in}\right)\right] \quad (23)$$

Exergy accumulation

$$Ex_{d,accum} = Ex_{d,f} - Ex_{d,i} = m_{total}\left[\left(u_{d,f} - u_{d,i}\right) - \left(s_{d,f} - s_{d,i}\right)\right] \quad (24)$$

Exergy destruction

$$\Delta Ex_{discharging} = Ex_{d,in} - Ex_{d,loss} - Ex_{d,accum} \quad (25)$$

Exergy efficiency

$$\psi_{discharging} = \frac{Exergy\ recovered\ by\ TES}{Exergy\ accumulated\ in\ TES} = \frac{Ex_{rec}}{Ex_{d,accum}} \quad (26)$$

Overall Energy and Exergy efficiency

Energy efficiency

$$\eta_{O,TES} = \frac{Energy\ recovered\ from\ TES\ during\ discharging}{Energy\ input\ to\ TES\ during\ charging} = \frac{\sum Q_{rec}}{\sum Q_{in,TES}} \quad (27)$$

Exergy efficiency

$$\psi_{O,TES} = \frac{Exergy\ recovered\ from\ TES\ during\ discharging}{Exergy\ input\ to\ TES\ during\ charging} = \frac{\sum Ex_{rec}}{\sum Ex_{c,in}} \quad (28)$$

3.4 Environmental Impact Analysis

With the ever-increasing concern about the environmental impact and specifically global warming due to greenhouse gases, it has become essential to evaluate and analyze the newly designed and developed system environmentally before heading forward. The developed system was weighed on an environmental impact basis which is quantified based on saving on carbon dioxide emissions. The change resulted in significant savings in CO_2 yearly and finally a lesser carbon footprint.

The annual social cost of CO_2 emission varies from one country to another. The cost of penalty for CO_2 emissions is calculated using the relation,

$$\dot{Z}_{env} = m_{co_2}.C_{co_2} \quad (29)$$

In above equation C_{co_2} is the cost of unit carbon dioxide production and it varies from 0.022 1.63 INR/kg to 9.62 INR per kg of CO_2 emissions. In our study, prices of developing countries have been chosen which is 3.7 INR/kg. Here m_{co_2} is the mass of CO_2 emission and has been calculated using emission conversion factor as follows:

$$m_{co_2} = \lambda . Power\ consumption\ in\ kWh \quad (30)$$

Where, λ is the emission conversion factor having a value of 0.968 kg/kWh. It is essential to mention that India's energy mix has been used to obtain the results. Here it is taken as 1 kWh_e leading to 0.968 kg of CO_2 production.

3.5 Economic Analysis

Whether cooling, heating, or power, every solar-based system has indirect benefits in terms of environmental protection, lower health costs, and global climate benefits, but never a decision on investment in renewable systems are made on this basis. Quite a few times, lawmakers provide incentives that may attract investment when looking to these social benefits. However, any system must sustain itself until its financial viability or beneficiary.

The fossil-based system is relatively cheaper in terms of initial cost but they have a higher recurring cost including regular energy billing, maintenance cost, etc. whereas the Solar-based system is characterized by a high initial cost and negligible operating cost. Therefore it is very much needed that the life cycle cost approach has to be adopted when comparing the solar-based systems with the conventional-based systems.

The concept of life cycle cost includes both the initial investment cost and year-to-year operating cost in making economic decisions. The life cycle cost of any energy system is the total of the following cost made in its life term:

1. The initial capital cost includes the cost of equipment, installation and land cost (if any).
2. Its running cost throughout its life.
3. Interest cost, if money is invested through borrowing.
4. Periodic maintenance cost of equipment or any miscellaneous cost.
5. Taxes
6. Salvage value, if any at the end of its life span.

The first cost includes all the costs of owning the equipment and normally is one time. It includes the cost of equipment, installation cost, and the cost of land, if applicable. On the other hand, operation and maintenance cost includes the cost incurred during the life cycle of the domestic water heating system year on year for operating the system which includes recurring electricity cost for operating the system. During the economic evaluation of any solar-based system, the initial investment made has to be weighted over the intended benefits in terms of heat, power, or cooling which the system is supposed to provide. Hence the present value of future anticipated benefits needs to be evaluated. Various financial performance parameters are analyzed over here, refer to Table 6.

Table 6 Indicators of Economical Analysis

Economical Analysis Indicators/Parameters	**Eq. No.**
Simple payback period (SPBP)	
$\text{SPBP}=\frac{CC}{CF}$	31
Discounted payback period (DPBP)	
$DPBP=\frac{ln\left(\frac{1}{1-\frac{CC*r}{CF}}\right)}{\ln(1+r)}$	32

Internal Rate of Return

$$0 = \sum_{n=1}^{N} \frac{CF_n}{(1+IRR)^n} + CI \quad (33)$$

Levelized Cost of Heating (LCOH)

$$LCOH = \frac{TLCC}{E_n}\left[\frac{1-(1+i)^{-n}}{i}\right] \quad (34)$$

4. Results and Discussion

4.1 Experimental Validation of Analytical Model

Figure 5 shows the schematic diagram of the setup discussed above. However, only a solar hot charging loop is considered in this present study. Data received from different RTD sensors, mass flow sensors, pyranometer, and ambient temperature thermocouple have been integrated into the data logger and then the performance of ET-CPC coupled with a hot storage tank is discussed by

It is observed from this experimental validation that relative difference is within the range of 3-8%. Hence, there is a good agreement between the values from this analytical model and experimental results.

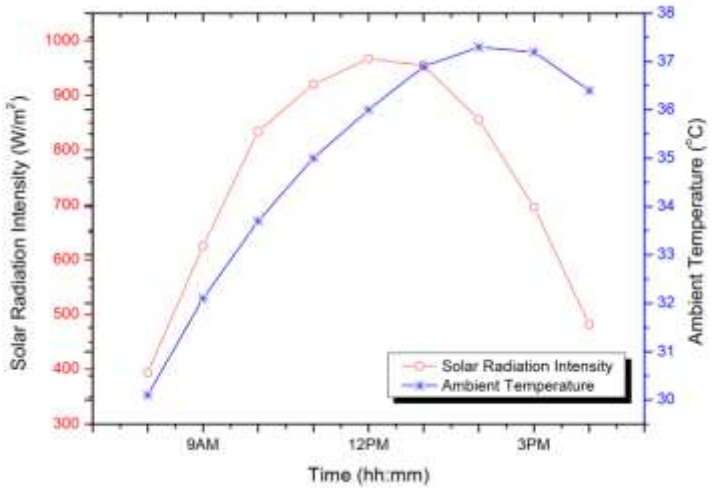

(a)

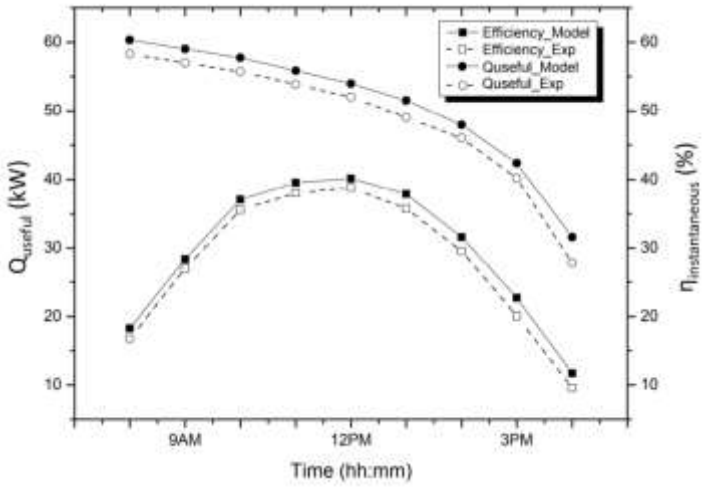

(b)

Figure 5 Experimental validation of analytical model on a typical day April 18, 2021 (a) Solar radiation intensity and ambient temperature (b) efficiency and Q_{useful} model and experimental

4.2 Parametric Analysis

This parametric study shows the effect of mass flow rate, solar radiation intensity and ambient temperature on the productivity and efficiency of the ET-CPC. A typical range of mass flow rate is taken from 0.0132 to 0.0357 kg/s through tubes of ET-CPC. The values of solar radiation intensity are considered from 200 to 1000 W/m^2 varying in the steps of 100 W/m^2. The ambient temperature values range from 27 to 43°C.

4.2.1 Effect of mass flow rate

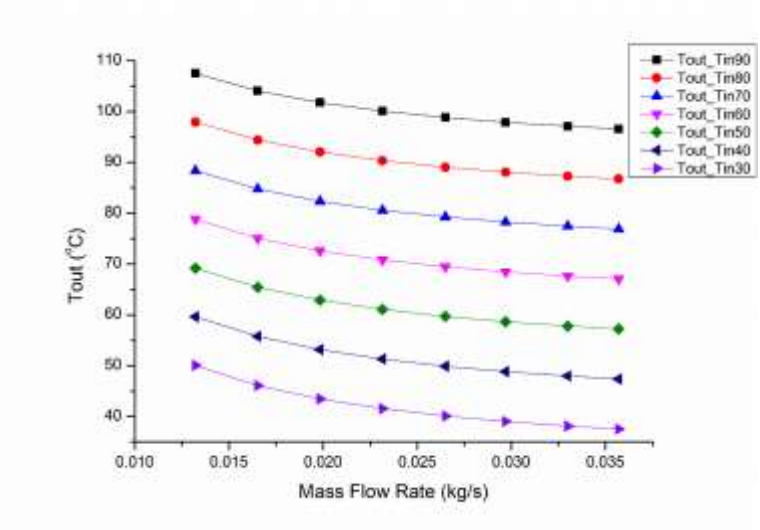

Figure 6 Effect of Mass Flow Rate on outlet temperature at a different inlet temperature

Figure 6 shows the variation of the system outlet temperature based on the mass flow rates. The solar radiation intensity has been kept at 1000 W/m^2 while the ambient temperature is kept at 27°C. Inlet temperatures have been varied from 30 to 90°C within the steps of 10°C. For the different inlet temperatures, the slopes of the curves are declining in nature, which also supports the theoretical knowledge. The slope of the curves decreases with the increase in inlet temperature. The slope of the curve for 30°C is steepest and the slope of the curve for 90°C inlet temperature is flattened.

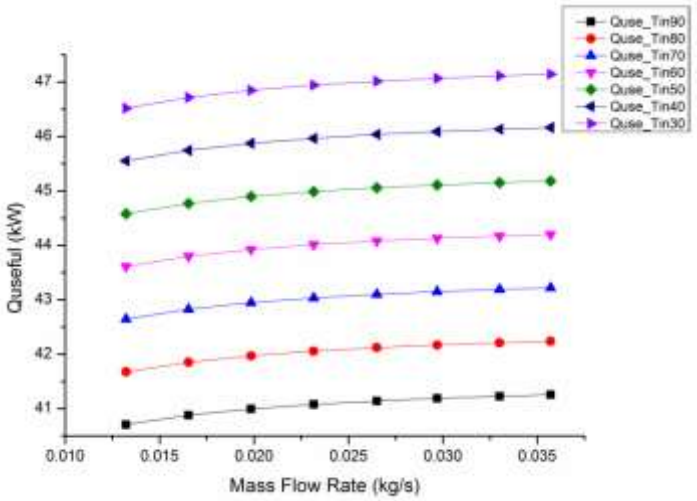

Figure 7 Effect of Mass Flow Rate on Q_{useful} at different inlet temperatures

Figure 7 shows the effect of mass flow rate over the useful heat gain for various inlet temperatures keeping solar radiation intensity 1000 W/m^2 and ambient temperature 27°C. Useful heat gain varies proportionally with the mass flow rate. Q_{useful} is higher for the lower inlet temperatures and vice-versa. At 30°C inlet temperature, the useful heat gain is highest and for 90°C inlet temperature, useful heat gain is lowest. This is since heat loss to the environment increases as the inlet temperature increases and lowers as the mass flow rate increases.

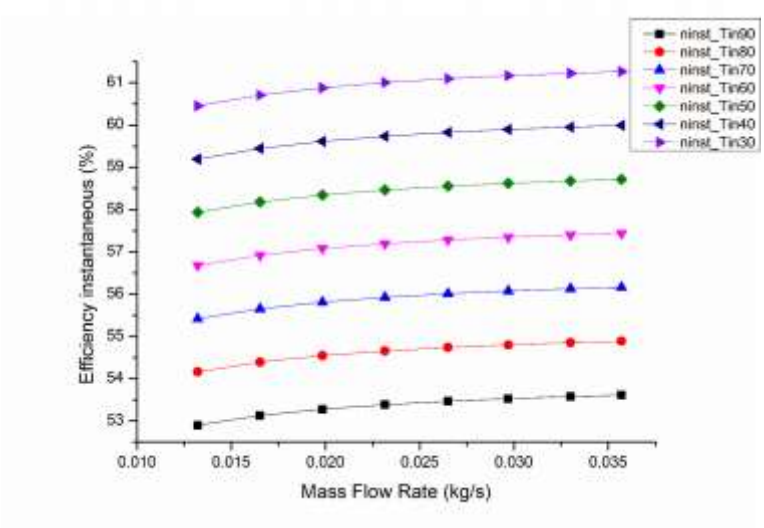

Figure 8 Effect of Mass Flow Rate on instantaneous efficiency with different inlet temperatures

Figure 8 shows the effect of mass flow rate over instantaneous efficiency of ET-CPC for various inlet temperatures at the solar intensity and ambient constant as described earlier. As the mass flow rate increases, the system's instantaneous efficiency is also increases and vice-versa. Instantaneous efficiency is better for lower inlet temperatures and reduces as temperature increases. The highest instantaneous efficiency is recorded at inlet temperature at 30°C and mass flow rate of 0.0357 kg/s.

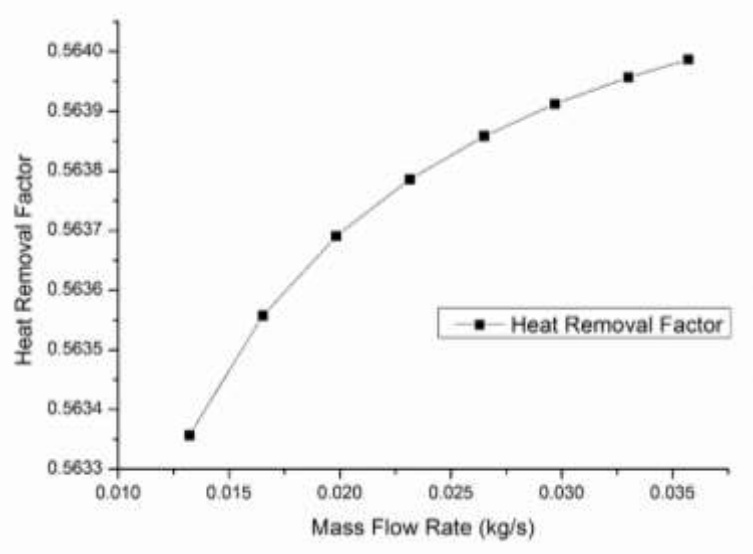

Figure 9 Effect of Mass Flow Rate on Heat Removal Factor

The heat removal factor is an important design parameter as it is a measure of thermal resistance encountered by the absorbed solar radiation is reaching the collector fluid**.** Figure 9 shows the effect of mass flow rate on the heat removal factor. This can be concluded that there is an increasing trend for heat removal factor, however, this increase in heat removal factor is not significant thus an average value of 0.5635 is taken for further evaluation.

4.2.2 Effect of solar radiation intensity

The effect of solar radiation intensity is quite essential to assess as an operating parameter since it is the base for any type of solar energy projects without which proper sizing and economics of

356 solar energy projects cannot be estimated. The effect of solar radiation intensity on outlet
357 temperature is shown in Figure 10. The solar radiation intensity is ranging from 200 to 1000 m^2
358 taking fluid inlet temperature of 27°C and a constant mass flow rate of 0.0357 kg/s. There is an
359 obvious increase in the fluid outlet temperature corresponding to the increase in the solar
360 radiation intensity. However, as the inlet temperature increases, the outlet temperature increases
361 proportionally with the solar radiation intensity.

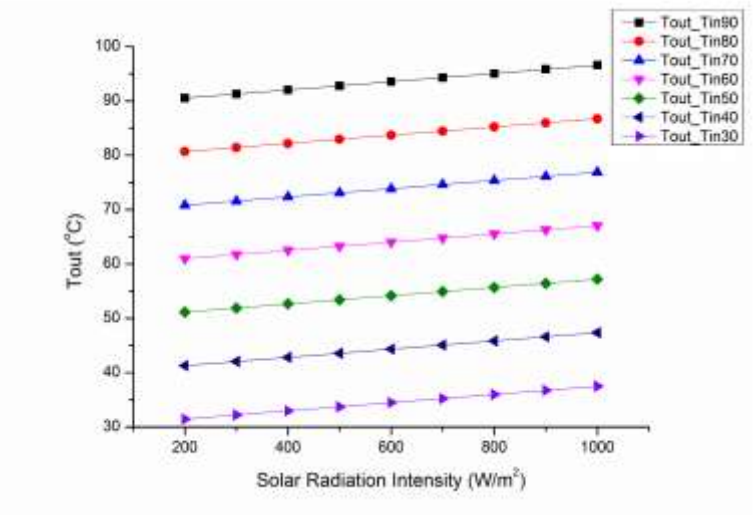

362

363 Figure 10 Variation of the outlet temperature as a function of the solar radiation intensity for
364 various inlet temperatures

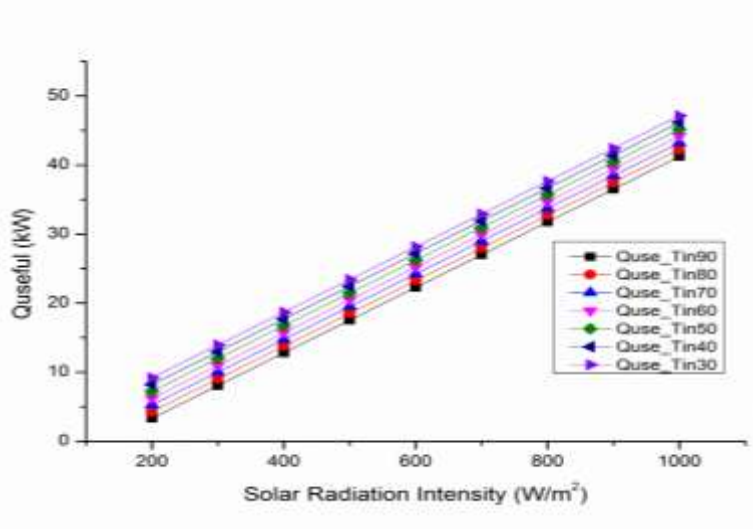

365

366 Figure 11 Effect of solar radiation intensity on useful heat gain

Figure 11 shows that solar radiation intensity's effect on useful heat gain for various inlet temperatures ranging from 30°C to 90°C. As mentioned earlier, while showing this mass flow rate is kept as 0.0357 kg/s, and ambient temperature is taken as 27°C. It can be noted from the figure that useful heat gain is directly proportional to the solar radiation intensity. For 30°C inlet temperature, the useful heat gain is highest and lowers as the inlet temperature increases. Useful heat gain is ranges between 40-46 kW for a given system's solar radiation intensity of 1000 W/m^2.

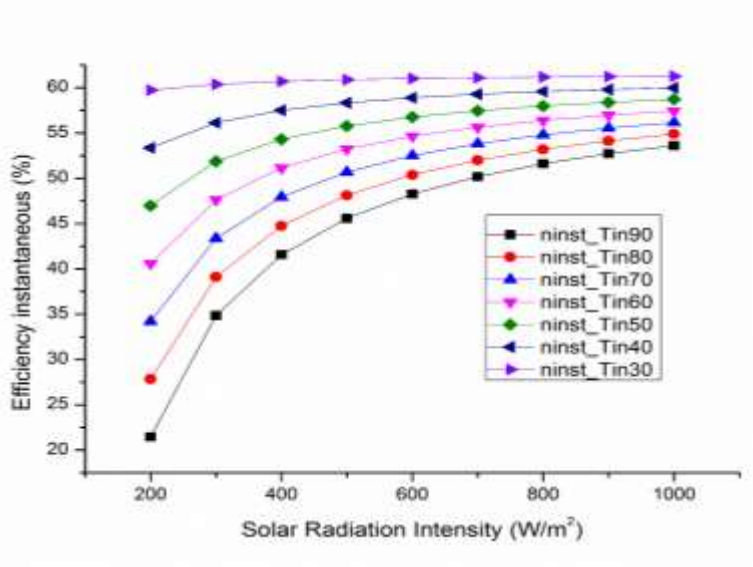

Figure 12 Effect of solar radiation intensity on instantaneous efficiency

Figure 12 represents the effect of solar radiation intensity on instantaneous efficiency for various inlet temperatures as discussed earlier. The instantaneous efficiency usually increases with the increase in the solar radiation intensity. The highest instantaneous efficiency was observed at 30°C inlet temperature at solar radiation intensity of 1000 W/m^2. As the inlet temperature of fluid increases, instantaneous efficiency decreases. This is mainly because of higher heat losses to the environment at higher inlet temperatures. However, these relative differences reduce at the

382 higher value of solar radiation intensity. Further, it can be observed that instantaneous efficiency
383 is still in the range of 40-50% which is significantly better than any other stationary STC.

384 **4.2.3 Effect of Ambient Temperature**

385 The effect of ambient temperature on productivity is reported in this section. The solar radiation
386 intensity is considered as 1000 W/m^2 along with a constant mass flow rate of 0.0357 kg/s. Figure
387 13 shows the effect of ambient temperature over fluid outlet temperature for various inlet
388 temperatures. It is observed that there is no significant variation observed in the fluid outlet
389 temperatures with ambient temperatures. Hence it can be concluded from this discussion that
390 ambient is the least dominant factor which affects the productivity of ET-CPC and further, useful
391 heat gain and instantaneous efficiency.

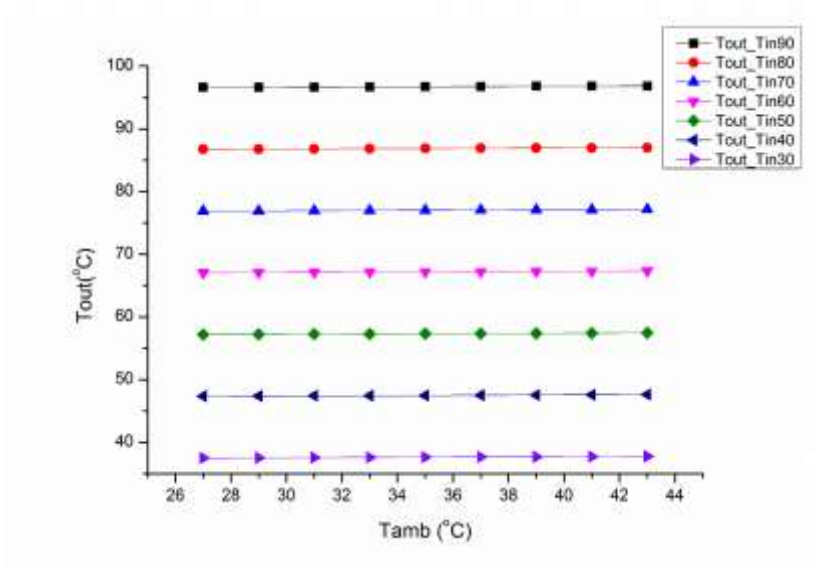

392

393 Figure 13 Effect of ambient temperature on Outlet temperature with different inlet temperatures

394 **4.3 Evaluation of Useful energy and exergy gain under actual meteorological conditions**

395 As mentioned earlier, four meteorological conditions of Rajasthan (India) have been considered.
396 Data have been recovered using the TMY2 file for these identified locations. The information
397 has been used in the model to evaluate the variation of productivity and efficiency for the stated

ET-CPC powered SDWH system with the help of various indicators of energy and exergy analysis such as useful heat gain, instantaneous efficiency, exergy gain, and exergetic efficiency. The results have been shown in stack form altogether to have a better and direct comparison of these identified indicators.

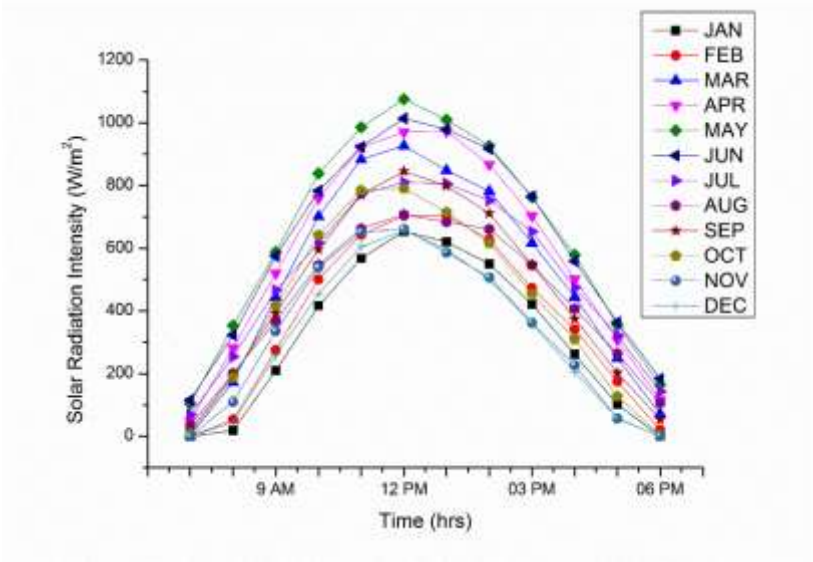

(a)

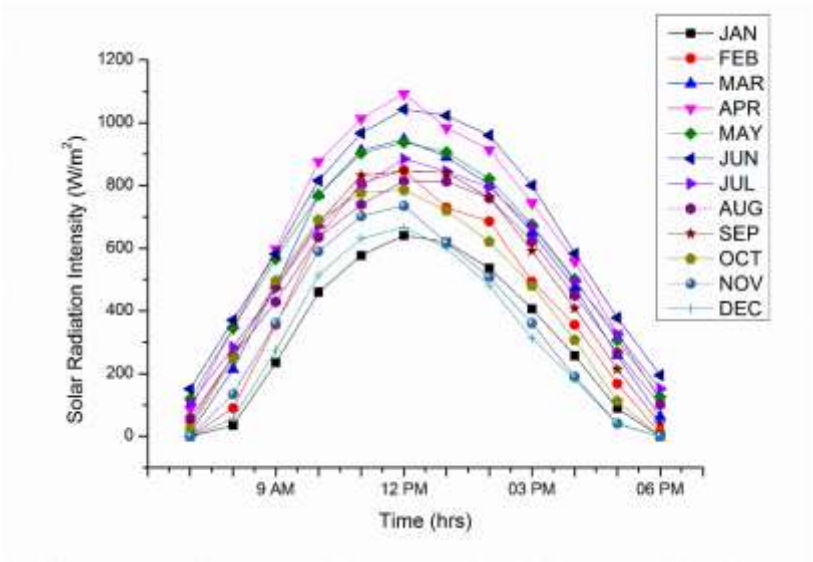

(b)

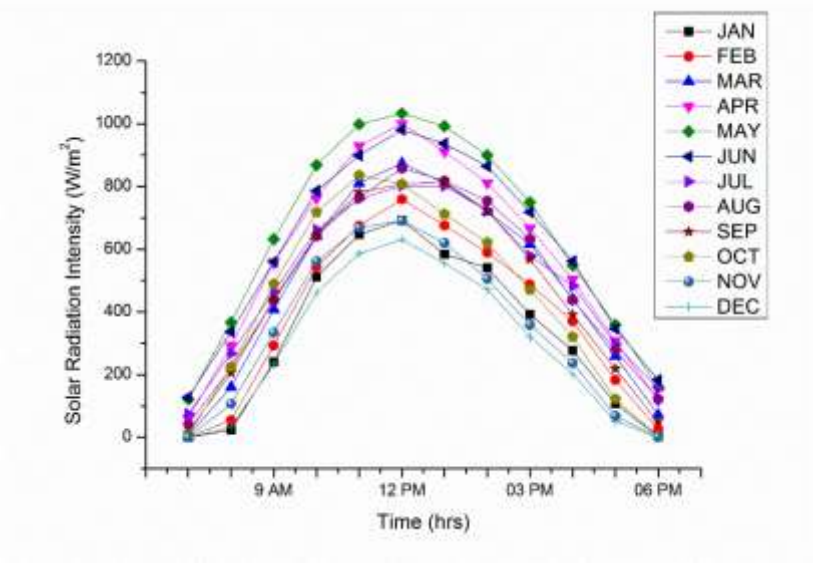

406

407 (c)

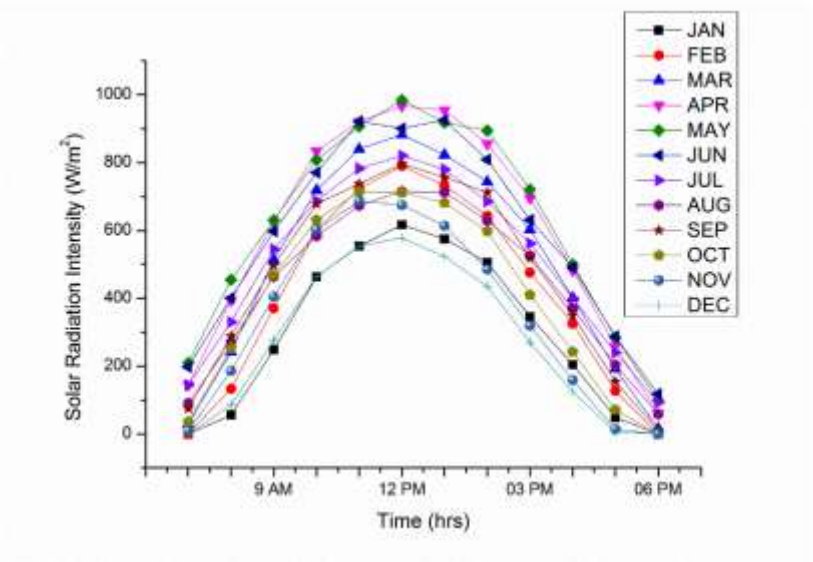

408

409 (d)

410 Figure 14 Radiation Intensity curves for (a) Barmer (b) Jodhpur (c) Jaisalmer (d) Jaipur

411 Figure 14 (a), (b), (c) and (d) shows the solar radiation intensity variation for year-round at
412 Barmer, Jodhpur, Jaisalmer, and Jaipur respectively. The highest solar radiation intensity data are
413 recorded between April and June while the lowest is recorded between November and January.
414 The highest solar intensity is observed around 12 PM for nearly every month. The highest value

of solar intensity is recorded as 1075, 1093, 1033 and 985 W/m^2 for Barmer, Jodhpur, Jaisalmer and Jaipur respectively.

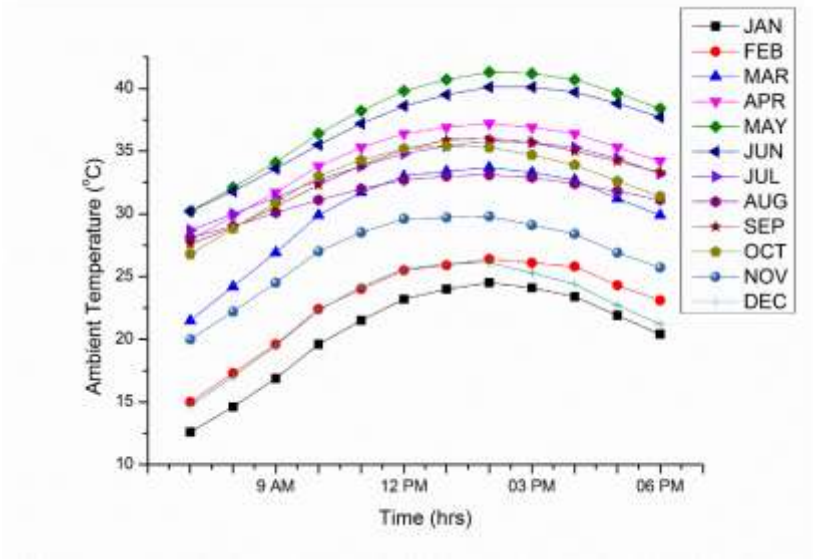

(a)

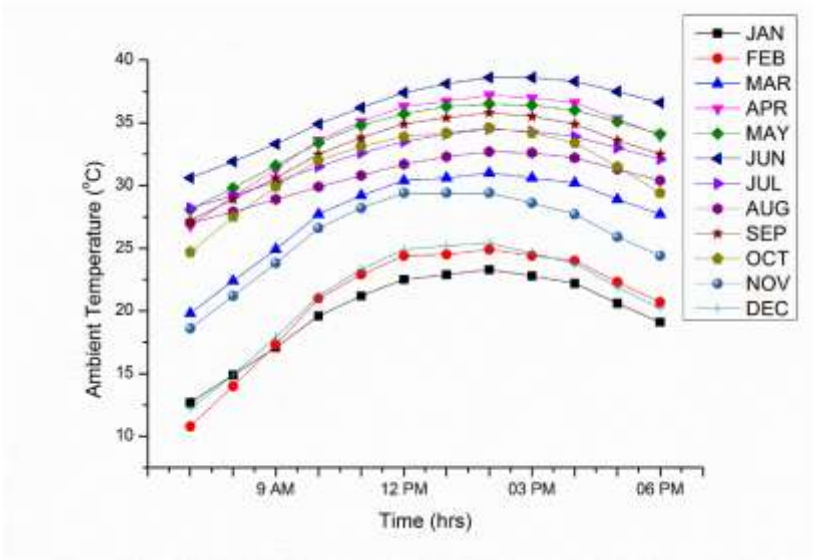

(b)

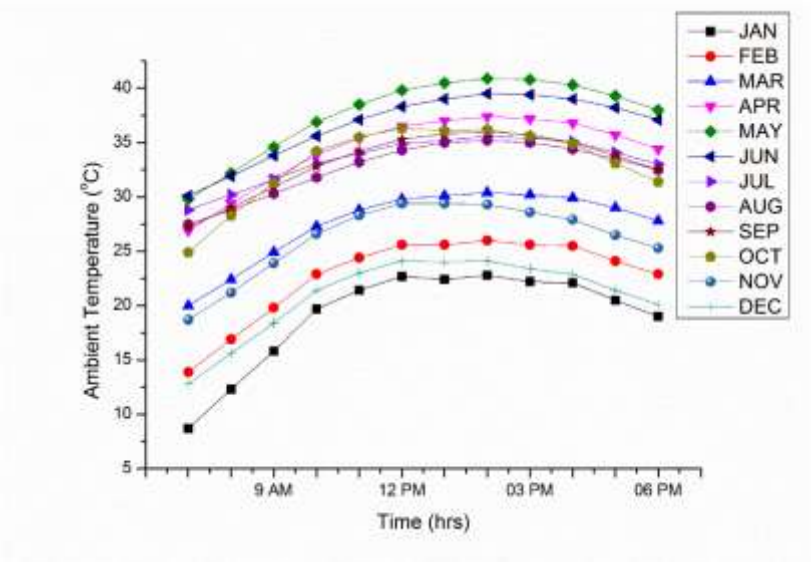

(c)

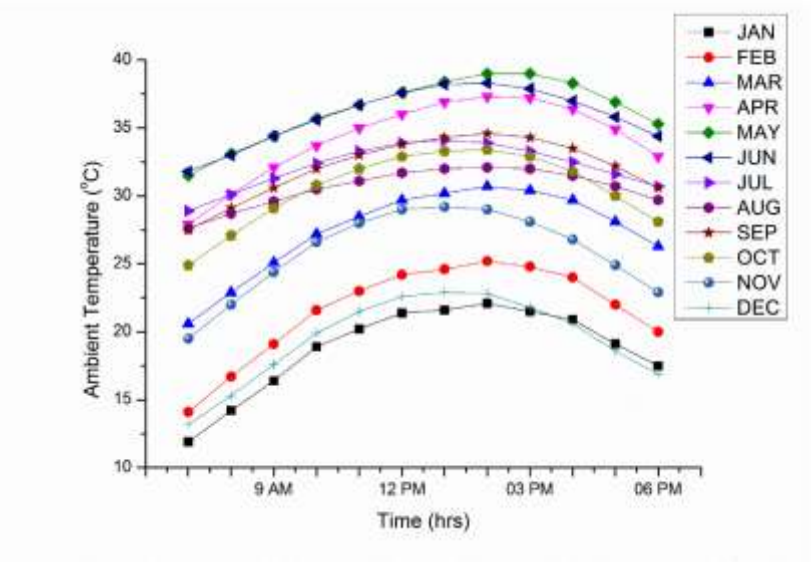

(d)

Figure 15 Ambient temperature curves for (a) Barmer (b) Jodhpur (c) Jaisalmer (d) Jaipur

Figure 15 (a), (b), (c), and (d) shows the variation of ambient temperature around the year for Barmer, Jodhpur, Jaisalmer and Jaipur respectively. It is observed that the highest ambient temperature achieved in the month may and lowest ambient temperature in the month January around 2 PM.]The highest ambient temperature was recorded as 41.3, 38.5, 40.9 and 39°C for

Barmer, Jodhpur, Jaisalmer and Jaipur respectively while the lowest temperature recorded was 15°C for Jaisalmer for a specified time of the day. The warmest months are May, June and July for all specified locations while the coldest months are December, January and February.

4.3.1 Energy Analysis

Figure 16 (a) shows a comparison analysis between the solar radiation intensity, useful heat gain and instantaneous efficiency under the meteorological condition of Barmer for the different-different months of a typical meteorological year (TMY). Similarly, Figures 16 (b), (c) and (d) are showing useful heat gain, instantaneous efficiency and solar radiation intensity for different months at locations Jodhpur, Jaisalmer and Jaipur respectively. The curve shows that the highest solar radiation intensity 1075 W/m^2 measured in May month. Similarly, the useful heat gain curve also has a higher value of 45.03kW during April and May. It is observed from the Figure that the solar radiation intensity and Q_{useful} are greater in the summer season months. But the instantaneous efficiency curve shows the higher values for the winter months. It is mainly because of the higher temperature difference between the inlet and outlet fluid in winter and efficiency is directly proportional to this temperature difference so the instantaneous efficiency is higher in December and January.

The highest value was measured as 67.25% in January. Similarly, the highest solar radiation intensity comes 1093 W/m^2 for Jodhpur followed by 1033 and 985 W/m^2 for Jaisalmer and Jodhpur locations during April and May. Accordingly, the Q_{useful} is measured higher for April, May and June. The highest value of Q_{useful} is recorded as 46.02 kW for Jodhpur followed by 42.86 and 40.67 kW for Jaisalmer and Jaipur respectively during April and June. However, as discussed earlier, the highest instantaneous efficiency of 66.64% for Jodhpur is recorded during January followed by 67.14 and 66.53% for Jaisalmer and Jodhpur respectively.

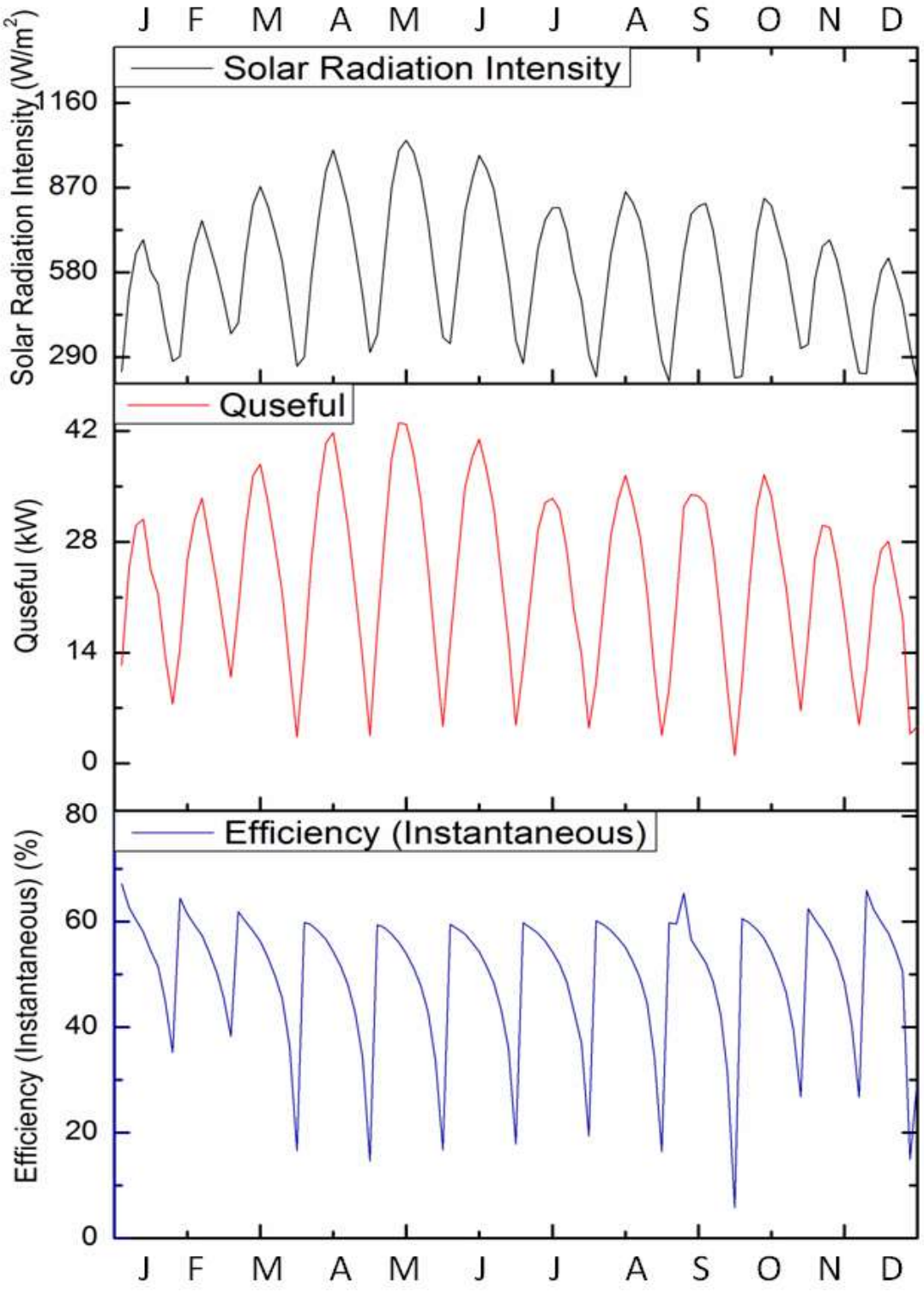
J F M A M J J A S O N D
Solar Radiation Intensity
Solar Radiation Intensity (W/m2)
1160
870
580
290
Quseful
Quseful (kW)
42
28
14
0
Efficiency (Instantaneous)
Efficiency (Instantaneous) (%)
80
60
40
20
0
J F M A M J J A S O N D

453

454 (a)

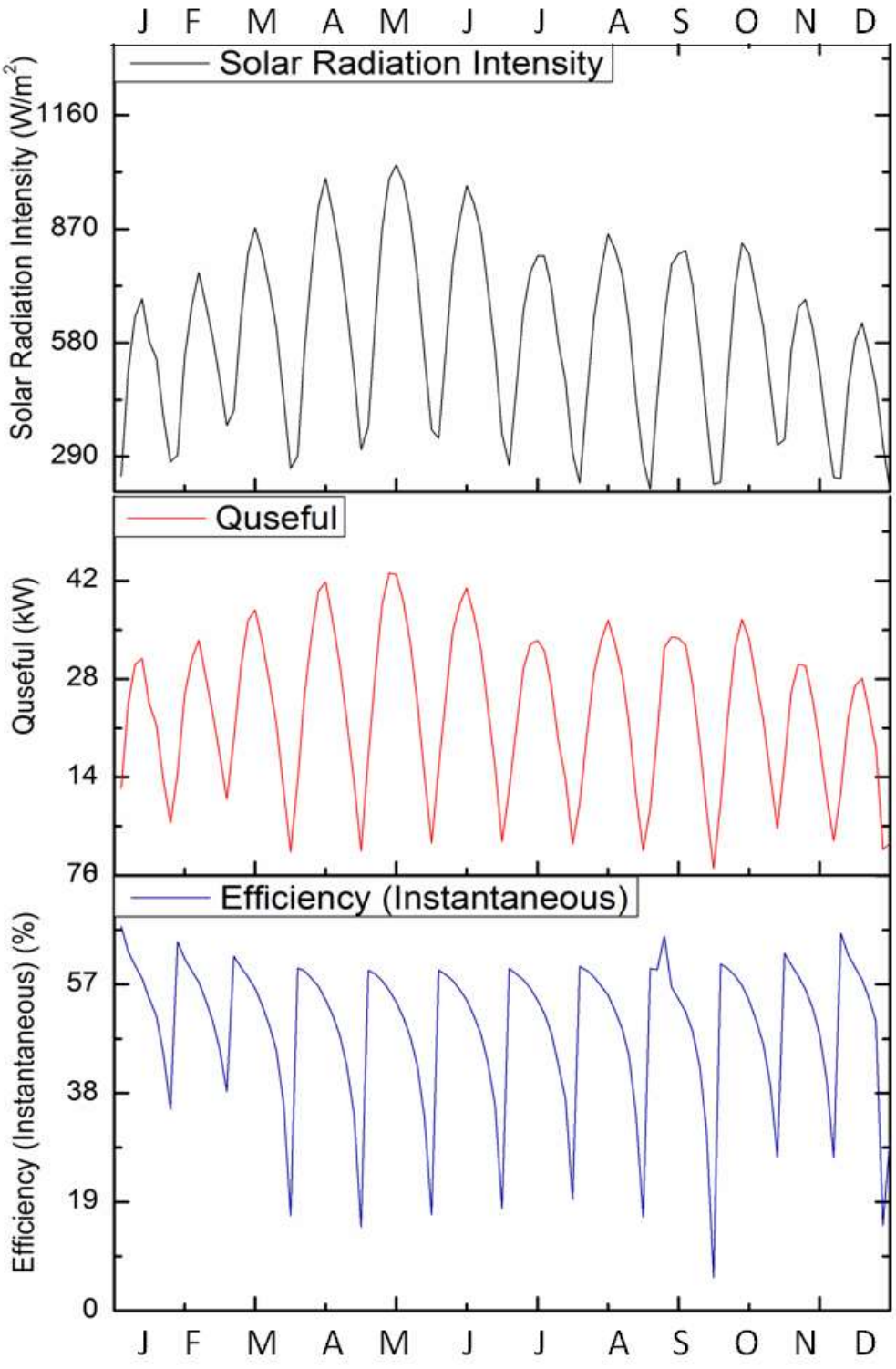
J F M A M J J A S O N D
Solar Radiation Intensity
Solar Radiation Intensity (W/m²)
1160
870
580
290
Quseful
Quseful (kW)
42
28
14
70
Efficiency (Instantaneous)
Efficiency (Instantaneous) (%)
57
38
19
0
J F M A M J J A S O N D

455

456 (b)

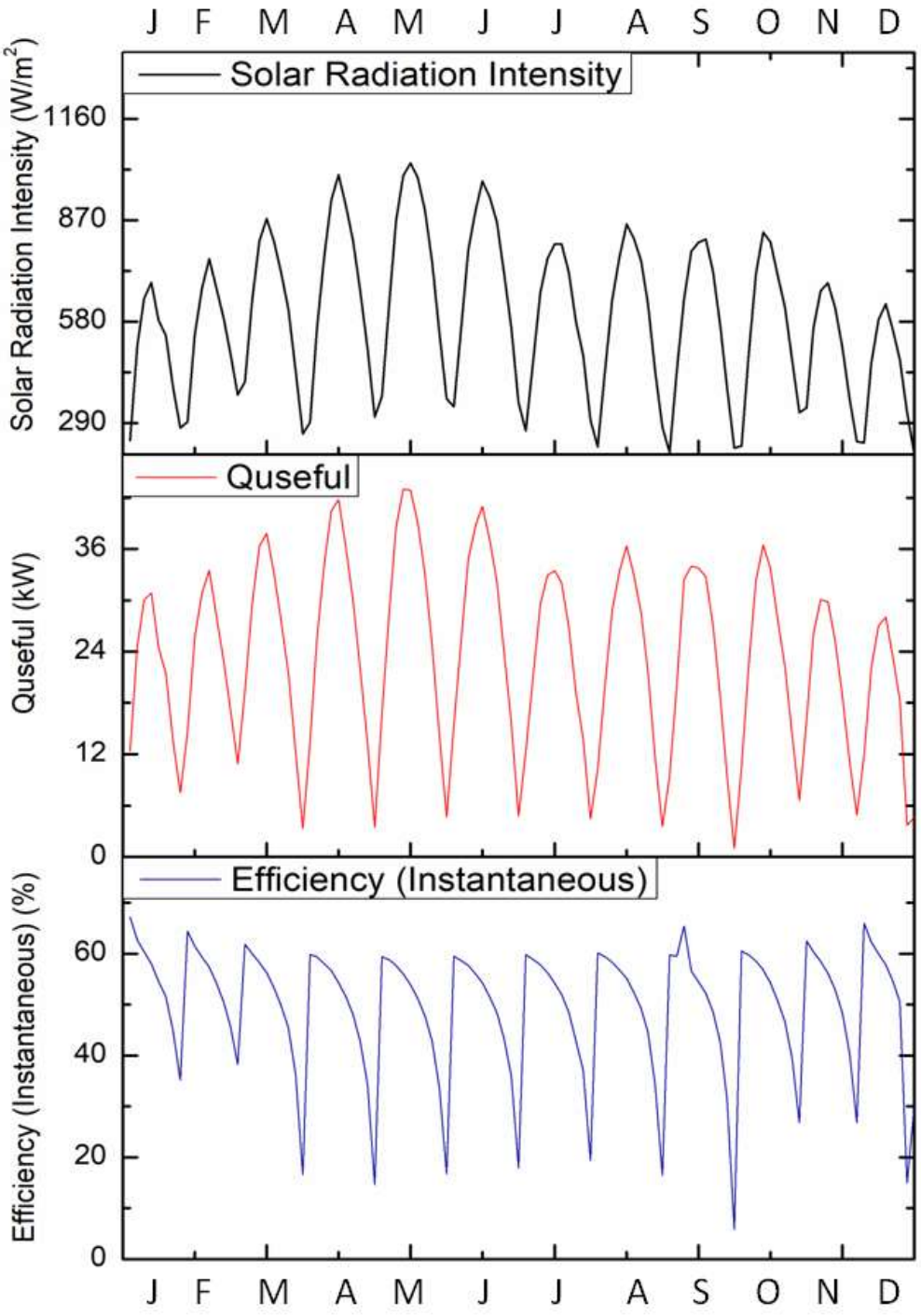
J F M A M J J A S O N D
Solar Radiation Intensity
Solar Radiation Intensity (W/m2)
1160
870
580
290
Quseful
Quseful (kW)
36
24
12
0
Efficiency (Instantaneous)
Efficiency (Instantaneous) (%)
60
40
20
0
J F M A M J J A S O N D

457

458 (c)

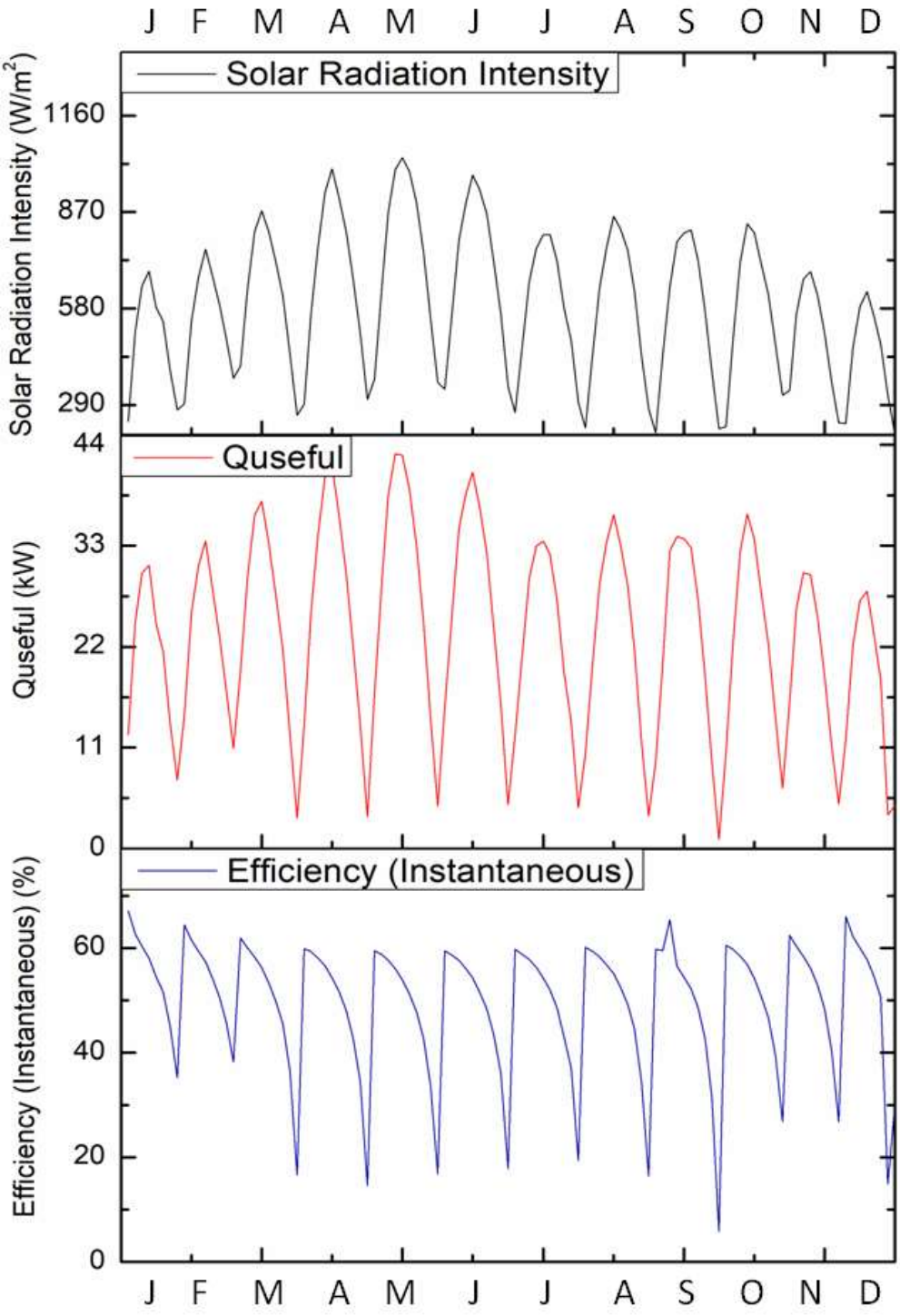

(d)

Figure 16 Parameters indicating Energy Analysis under meteorological condition of (a) Barmer (b) Jodhpur (c) Jaisalmer (d) Jaipur

4.3.2 Exergy analysis

Figure 17 (a), (b), (c) and (d) manifests the exergy analysis consisting of three parameters as amount of exergy inlet, amount of useful exergy and exergetic efficiency for various months under the meteorological conditions of Barmer, Jodhpur, Jaisalmer and Jaipur respectively. The first part of the curves elucidates the exergy variation in other months. The maximum exergy in measured as 80.74 kW during May month. This curve also illustrates that the amount of exergy is higher in the summer season and lower in the winter season. It is mainly because of the higher solar radiation intensity in summers as compared to the winters. The second and third parts of these curves illustrate the behavior of exergy gain and exergetic efficiency for different specified locations during different months. The highest value of exergy gain is observed during April and June. It is observed as 7.50 kW for Jodhpur followed by 7.33, 7.17 and 7.09 kW for Barmer, Jaisalmer and Jaipur respectively during May. The exergetic efficiency is observed as 10.57% for Barmer during May. Since the amount of exergy useful is higher and subsequently exergetic efficiency is also higher. The highest exergetic efficiency is again recorded for Jodhpur as 11. 05% during June. The highest exergetic efficiency for Jaisalmer and Jaipur is recorded as 10.58 and 10.55% respectively.

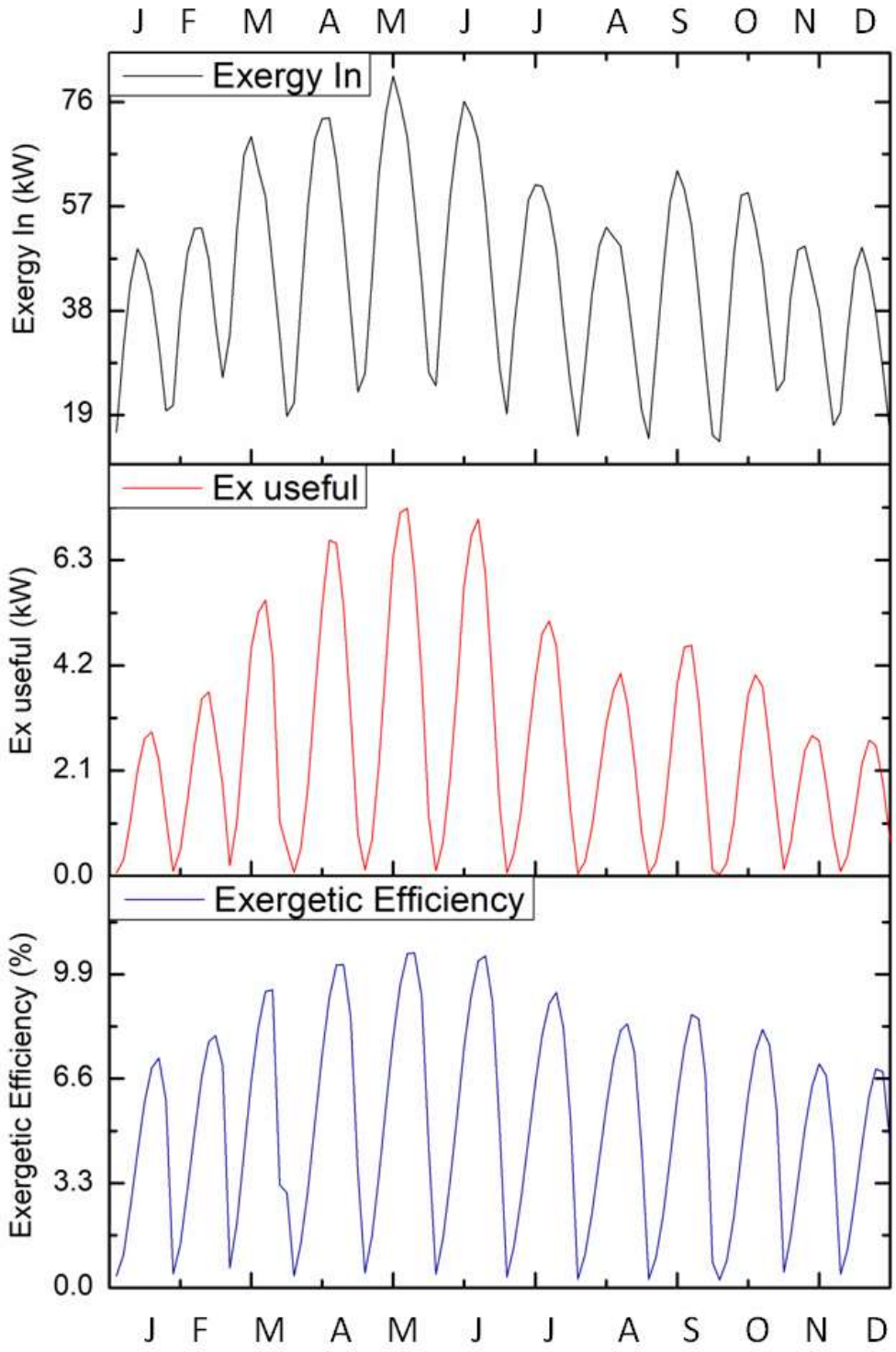
J F M A M J J A S O N D
Exergy In
Exergy In (kW)
76
57
38
19
Ex useful
Ex useful (kW)
6.3
4.2
2.1
0.0
Exergetic Efficiency
Exergetic Efficiency (%)
9.9
6.6
3.3
0.0
J F M A M J J A S O N D

479

480 (a)

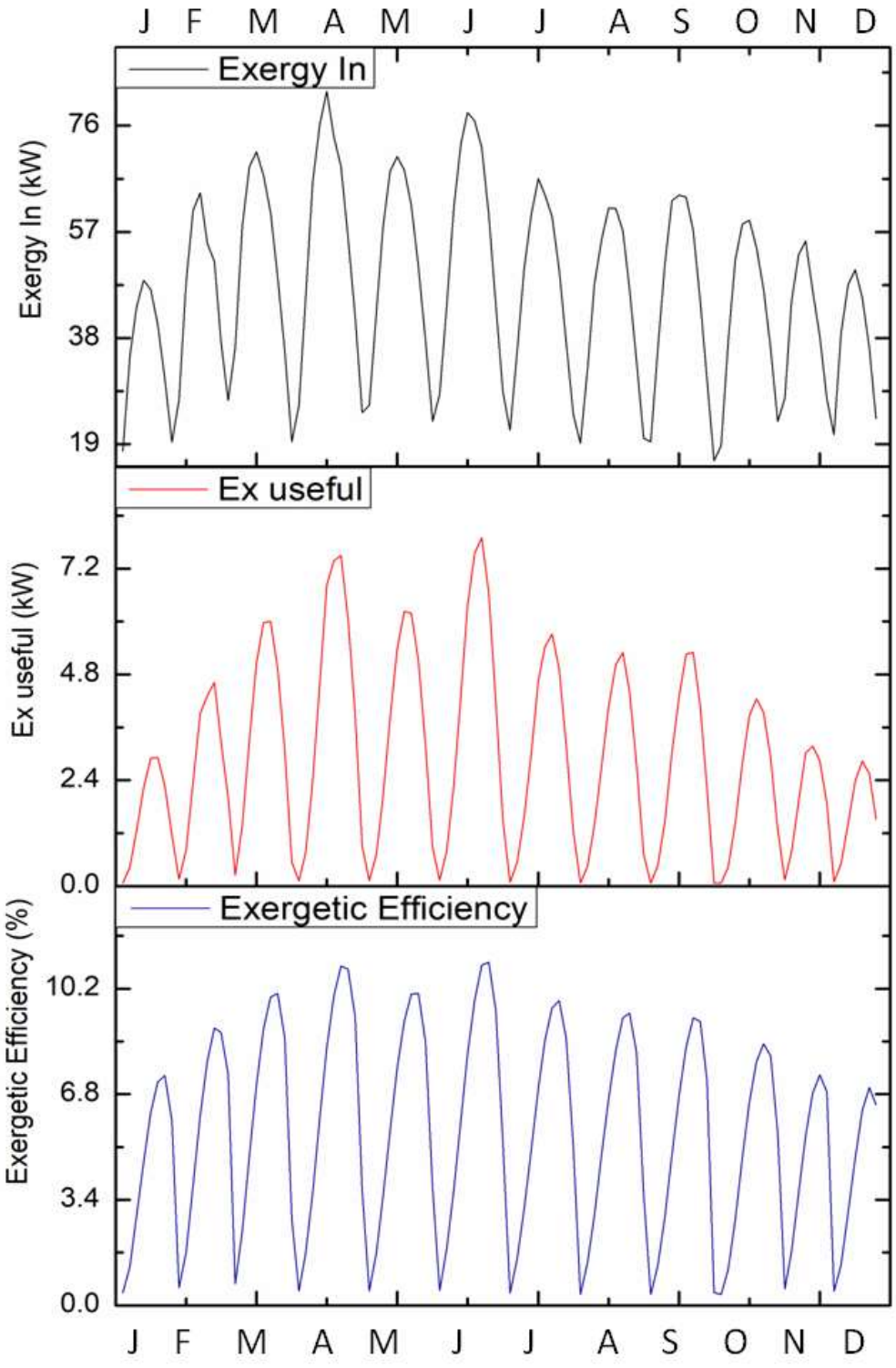
J F M A M J J A S O N D
Exergy In
Exergy In (kW)
76
57
38
19
Ex useful
Ex useful (kW)
7.2
4.8
2.4
0.0
Exergetic Efficiency
Exergetic Efficiency (%)
10.2
6.8
3.4
0.0
J F M A M J J A S O N D

481

482 (b)

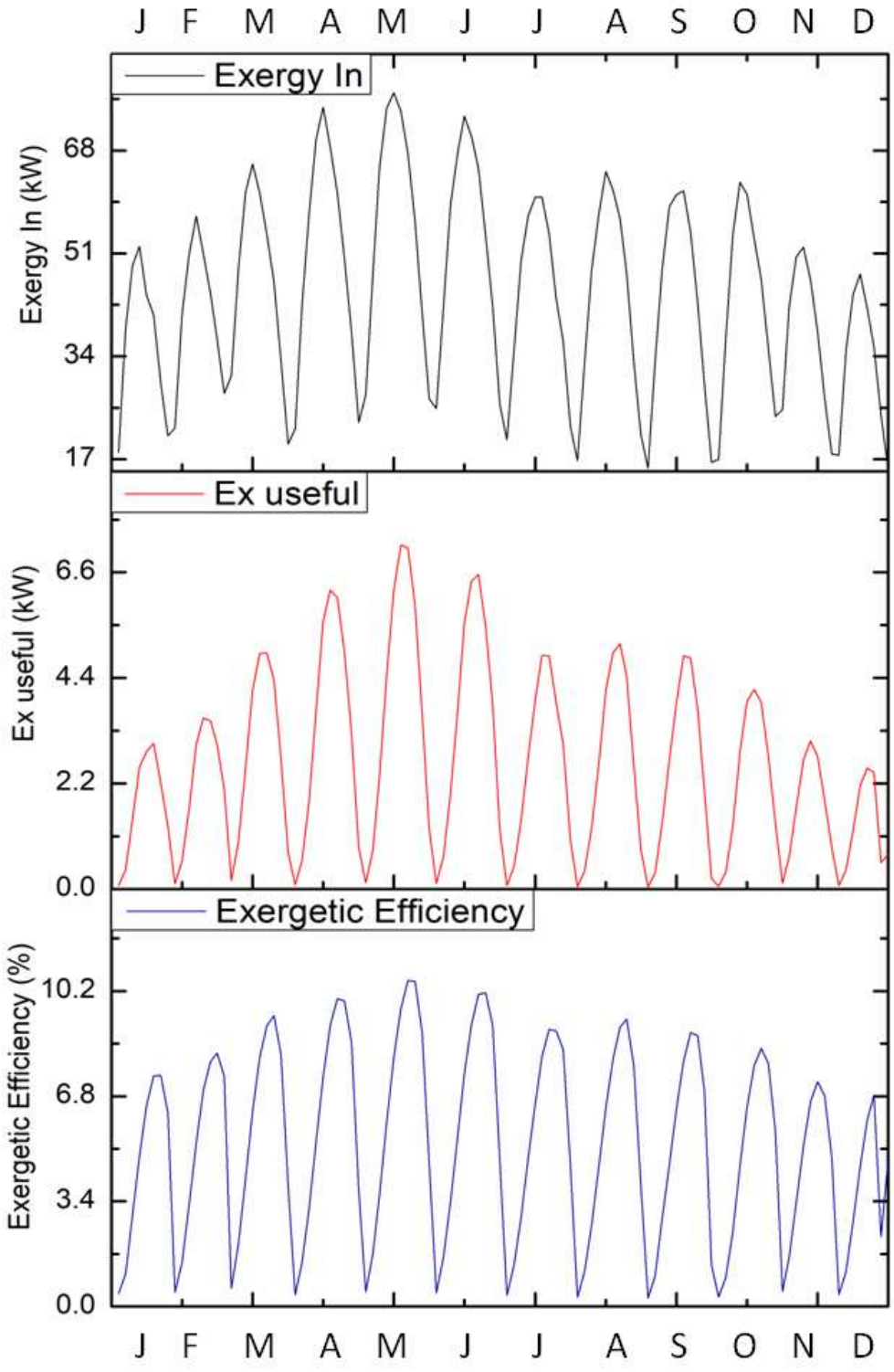
J F M A M J J A S O N D
Exergy In
Exergy In (kW)
68
51
34
17
Ex useful
Ex useful (kW)
6.6
4.4
2.2
0.0
Exergetic Efficiency
Exergetic Efficiency (%)
10.2
6.8
3.4
0.0
J F M A M J J A S O N D

483

484 (c)

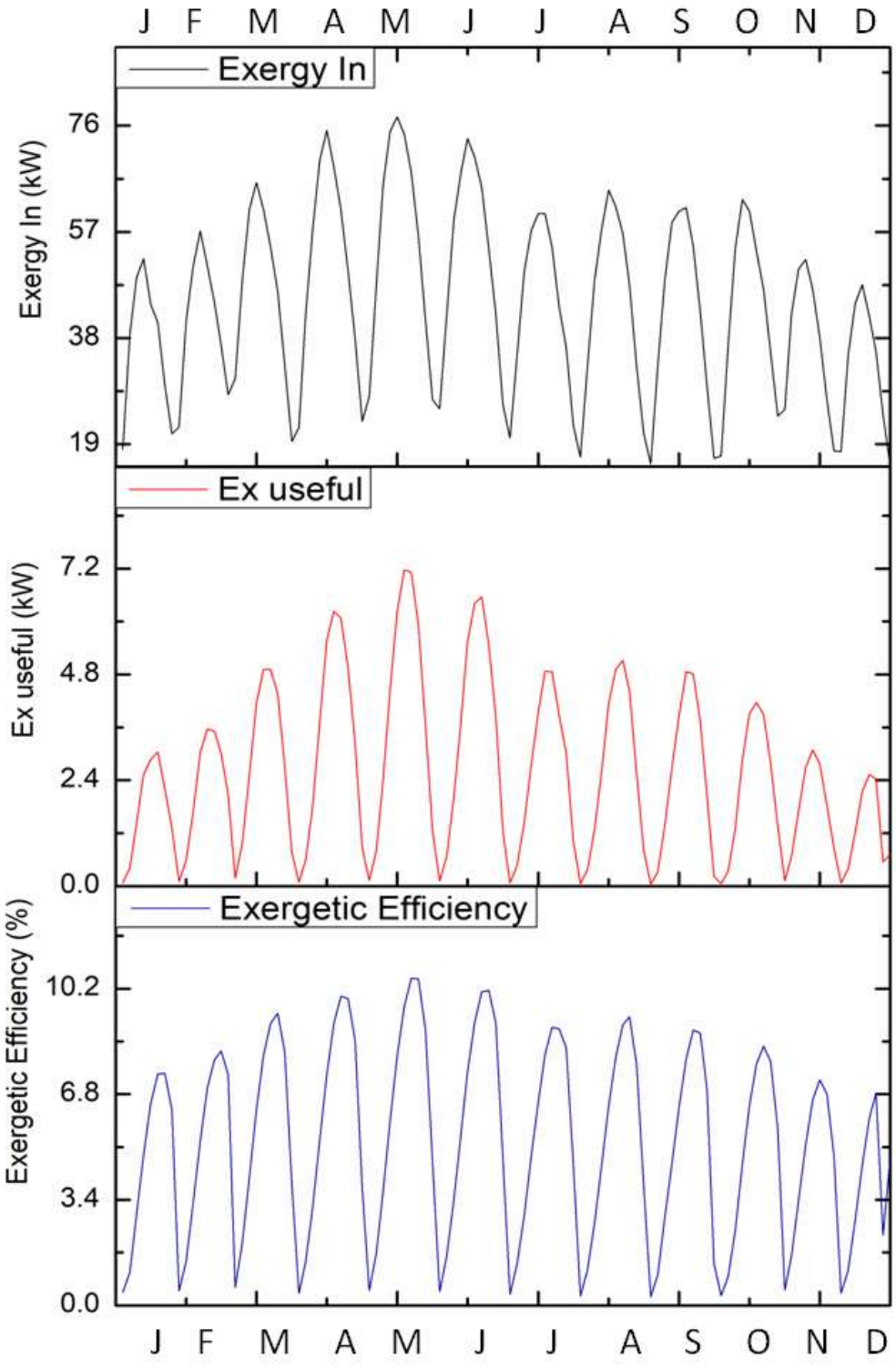

(d)

Figure 17 Parameters indicating Exergy Analysis under meteorological condition of (a) Barmer (b) Jodhpur (c) Jaisalmer (d) Jaipur

However, a comparison is essential to discuss site selection to indicate the annual useful heat gain and useful exergy gain for all specified locations. Figure 18 shows the comparison of solar energy received by the ET-CPC solar field, useful heat gain, exergy inlet and exergy gain annual for the specified locations Barmer, Jodhpur, Jaipur and Jaisalmer. As observed Jodhpur is having the most excellent solar radiation 162 MWh/year and thus highest annual useful energy and exergy gain as reported to be 79.72 MWh and 9.311 MWh annually. Jaisalmer receives 157.85 MWh of solar radiation per year which is getting converted to 76.90 MWh/year of useful heat gain. Exergy gain calculated for Jaisalmer is 8.53 MWh concerning inlet Exergy of 146.63 MWh per year. Similarly for useful heat gain is as 75.92 and 75.32 MWh/year for Barmer and Jaipur respectively. Exergy gain for Barmer and Jaipur is calculated as 8.4 and 8.32 MWh/year respectively.

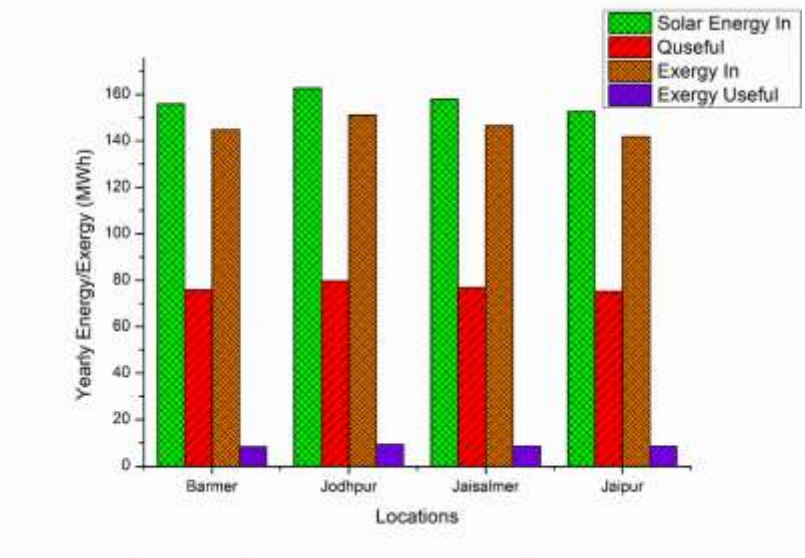

Figure 18 Solar energy-exergy graph comparison for four different meteorological condition

4.4 Environmental Impact Analysis

The use of solar energy is always helpful to overcome CO_2 emission-related environmental impact issues such as global warming, smog, acid rain and rise in mean global ambient

temperature. This analysis reports the massive savings of CO_2 emission compared to the other existing conventional solar water heating systems. Figure 19 represents the CO_2 emission saved in kg of CO_2 for various identified locations.

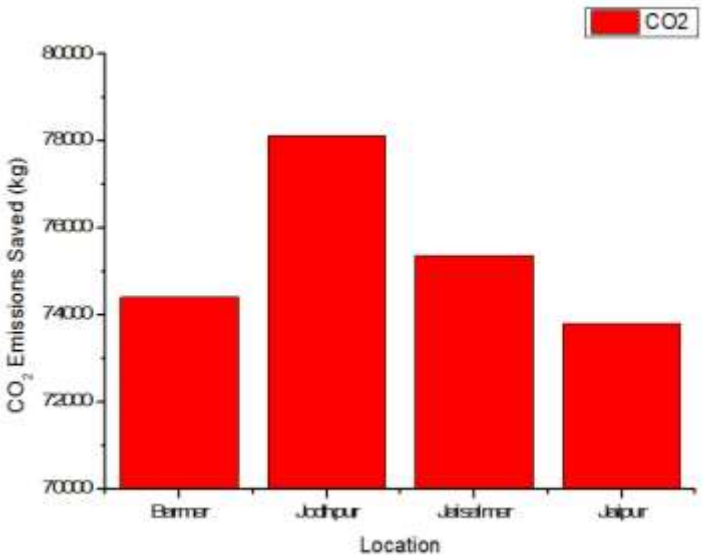

Figure 19 Comparison of CO_2 emission saved with the use of solar energy for identified locations

4.5 Economic Analysis

As discussed earlier, economic analysis is quite an essential to compare different existing technologies based on profitability. A detailed economic analysis has been reported here to understand the effect of location on cost recovery and other indicators of economic profitability. There are five conventional fuels-based water heating systems for the economic comparison with the existing solar water heating system. Table 7 shows the different fuels used for water heating and their corresponding price, conversion efficiency and calorific value of fuels.

Table 7 Comparison of price, conversion efficiency and calorific values for various fuels

Sr. No.	Fuel	Units	Price	Conversion Efficiency	CV Fuel (MJ/kg)
1	Electricity	per kWh	9.84	0.9	3.6 (MJ/unit)
2	LPG	per kg	86.34	0.6	55

3	Karosene	per kg	67.68	0.4	45
4	Fuelwood	per kg	10	0.25	22
5	Natural gas	per kg	34.2	0.6	50

519 Table 8 shows the installation cost or first cost of the different water heating systems. It can be
520 easily identified that the first cost of a solar water heating system is significantly higher than
521 those of other systems. Table 9 reports the annual operation and maintenance cost of various
522 fuels while Table 10 shows the estimated life expectancy of the selected systems. Economic
523 evaluation is done based on equations reported in Table 6. Table 11 describes the internal rate of
524 return and payback periods. The internal rate of return is 16.82% for Jodhpur followed by 16.77,
525 16.76 and 16.75 for Jaipur, Barmer and Jaisalmer respectively. Similarly simple payback period
526 is 4.49, 4.65, 4.72 and 4.75 years for Jodhpur, Jaipur, Barmer and Jaisalmer respectively. The
527 discounted payback period is also calculated which is ranging from 6.6 to 7.09 years similarly
528 for identified locations.

529 Table 8 Comparison of First Cost for various water heating systems

System	**First Cost in INR**
ET-CPC Solar Water Heating	947520
Electricity based Water Heater	250000
LPG/Kerosene/CNG operated water heaters	226762
Firewood operated water heater	250000

530

531 Table 9 O&M cost for various locations for different fuels

Sr. No.	**Fuel**	**Units**	**Price**	**Conversion Efficiency**	**CV Fuel (MJ/kg)**	**O&M Cost (INR)**			
						Barmer	**Jodhpur**	**Jaipur**	**Jaisalmer**
1	Electricity	per	9.84	0.9	3.6	830043	871598	873202	823490

		unit			(MJ/unit)				
2	LPG	per kg	86.34	0.6	55	715074.16	750875.4	724408.3	709432.2
3	Kerosene	per kg	67.68	0.4	45	1027639.6	1079090	1041054	1019532
4	Fuelwood	per kg	10	0.25	22	496924.36	521803.6	503410.9	493003.6
5	Natural gas	per kg	34.2	0.6	50	311571.58	327170.9	315638.6	309113.3

532

533 Table 10 **Life expectancy of equipment**

Expected Life (Solar System)	**15 years**
Expected Life (Electricity heating system)	15 years
Expected Life (LPG/CNG/Kerosene fired heating system)	15 years
Discount Rate	6% annual

534

535 Table 11 Comparison of IRR and payback periods for identified locations for solar water heating
536 system

	IRR(%)	**SPBP (Yr)**	**DPBP (Yr)**
Barmer	16.76	4.7169	7.024
Jodhpur	16.82	4.492	6.615
Jaipur	16.77	4.656	6.912
Jaisalmer	16.75	4.7543	7.093

537 A comparison of operation and maintenance costs has been presented in Figure 20. The kerosene
538 fuel-operated water heating system shows the highest cost of operation and maintenance,
539 followed by Electricity and LPG. This can be seen that solar energy is having significantly less
540 operation and maintenance costs as compared to that of other conventional fuels reported.

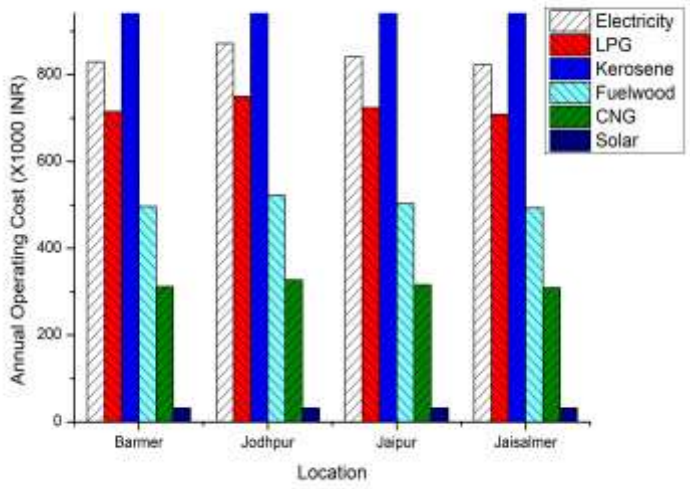

Figure 20 Comparison of Annual O&M cost for various fuels used for domestic water heating system

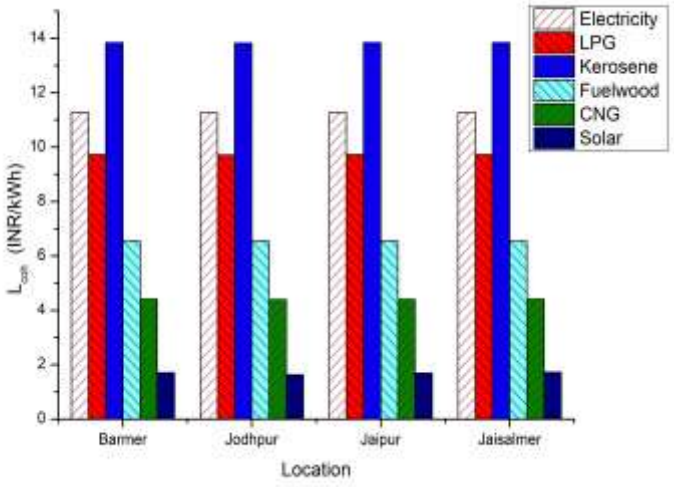

Figure 21 Comparison of Levelized cost of Heating for various fuels for identified locations

Levelized cost of Heating is essentially a significant indicator to compare overall cost per unit kWh of Heating. It can be seen from Figure 21, LCOH is significantly less in the case of ET-CPC solar water heating system ranging from 1.65 INR/kWh to 1.72 INR/kWh followed by Kerosene (13.83 INR/kWh) and Electricity (11.25 INR/kWh). SPBP and DPBP are calculated as

551 4.5-4.75 year and 6.6-7 year respectively taking a discount rate of 6%. The internal rate of return
552 is reported to be 16.76, 16.82, 16.77 and 16.75% for Barmer, Jodhpur, Jaipur and Jaisalmer
553 respectively which proved that it is a very profitable business model, refer to Table 11.

554 ## 5. Conclusion

555 An SDWH powered by an 81 m^2 ET-CPC solar collector field is reported in presented here.
556 Energy, exergy, environmental and economic analysis is carried out. The following points are
557 drawn as the conclusion of this work.

558 • The developed model results are validated with the experimental results and relative
559 differences are ranged from 3 to 8%.

560 • Parametric analysis shows that with the increase in mass flow rate ranging from 0.0132 to
561 0.0357 kg/s, there is simultaneous improvement in the useful heat gain and instantaneous
562 efficiency of ET-CPCs. However, there is a drop in the useful heat gain and instantaneous
563 efficiency with an increase in the inlet temperature which ranged from 30-90°C.

564 • Effect of solar radiation intensity ranging from 200 – 1000 W/m^2 has been reported for
565 various inlet temperatures to evaluate and compare the useful heat gain and instantaneous
566 efficiency of ET-CPC solar field.

567 • It has also been reported that there is no significant effect of ambient temperature over
568 the useful heat gain and efficiency.

569 • The analytical model is then implemented under meteorological conditions of four
570 specified locations (Barmer, Jodhpur, Jaisalmer and Jaipur), then annual energy and
571 exergy gain have been evaluated and compared. Jodhpur is receiving the most excellent

572 solar radiation and thus highest annual useful energy and exergy gain have been reported
573 to be 79.72 MWh and 9.311 MWh followed by Jaisalmer, Barmer and Jaipur.

574 • The economic analysis reports the simple payback period ranging from 4.5 to 4.75 years
575 and discounted payback period ranging from 6.6 to 7 years based on a 6% discount rate.

576 • Along with this, based on levelized cost of heating using solar energy as fuel is ranging
577 from 1.62 to 1.72 INR/kWh of heat compared to closest with the use of CNG as fuel
578 which is ranging from 4.39 to 4.41 INR/kWh.

579 • The highest LCOH has been reported for electricity for domestic water heating which
580 ranged from 11.25 to 11.27 INR/kWh.

581 • The internal rate of return is reported to be 16.76, 16.82, 16.77 and 16.75% for Barmer,
582 Jodhpur, Jaipur and Jaisalmer respectively which proved that it is a very profitable
583 business model.

584 • The environmental analysis also supports the previous trends and report 74400, 78125,
585 75371 and 73813 kg of CO_2 saved which anyway got added to the environment if the
586 electricity was used for the same purpose.

587 Hence it can be recommended that ET-CPC is a viable, economical and pollution-free alternative
588 to meet the medium temperature heat demand such as in solar water heating systems for
589 domestic and community use. ET-CPC operation is not possible during weak sunshine (<200
590 W/m^2) hours and technology advancement is needed in this direction. The use of nanofluids as a
591 working fluid is reported to be advantageous to improve the productivity and performance of the
592 ET-CPC further but insufficient data is there and that also reports operational issues. Research
593 could be made to find the optimal configuration of nanofluids to offer less/no operational issues

and optimal performance. Further, ET-CPC life cycle cost assessment could be worked out to understand the overall impact on nature.

-Ethical Approval

We confirm that this work has not been published elsewhere, nor it is currently under consideration for publication elsewhere.

-Consent to Participate

Authors give their consent to participate.

-Consent to Publish

We consent it to publish in the Environmental Science and Pollution Research after acceptance.

-Authors Contributions

Dinesh Kumar Sharma is a corresponding of this manuscript. He has involved in the development of entire manuscript.

Prof. Dilip Sharma has involved in the conceptualization of this research and reviewed the technical details of the manuscript.

Prof. Ahmed Hamza H Ali has involved in the conceptualization and reviewed the language and grammar of the manuscript.

-Funding

There are no funding disclosures to make.

-Competing Interests

Authors have no conflict of interest to disclose.

-Availability of data and materials

Calculations data and other relevant material would be made available to editor/reviewer as and when required.

References

Battisti R, Corrado A (2005) Environmental assessment of solar thermal collectors with integrated water storage. Journal of Cleaner Production 13:1295–1300. doi: 10.1016/j.jclepro.2005.05.007

Bejan A, Kearney DW, Kreith F (1981) Second law analysis and synthesis of solar collector systems. Journal of Solar Energy Engineering Transactions of ASME 103:23-28. doi: 10.1115/1.3266200

Bellos E, Tzivanidis C, Tsifis G (2017) Energetic, Exergetic, Economic and Environmental (4E) analysis of a solar assisted refrigeration system for various operating scenarios. Energy Conversion and Management 148:1055–1069. doi: 10.1016/j.enconman.2017.06.063

Caliskan H (2017) Energy, exergy, environmental, enviroeconomic, exergoenvironmental (EXEN) and exergoenviroeconomic (EXENEC) analyses of solar collectors. Renewable and Sustainable Energy Reviews 69:488–492. doi.org/10.1016/j.rser.2016.11.203

Cengel YA, Boles MA (2019) Thermodynamics: An Engineering Approach 9th Editon (SI Units). McGraw Hill Publication. Newyork

Chopra K, Tyagi V V., Pandey AK, et al (2021) Energy, exergy, enviroeconomic & exergoeconomic (4E) assessment of thermal energy storage assisted solar water heating system: Experimental & theoretical approach. Journal of Energy Storage 35:102232. doi: 10.1016/j.est.2021.102232

Dincer I, Rosen MA (2007) Exergy: Energy, environment and sustainable development. John Wiley and Sons

Faizal M, Saidur R, Mekhilef S, et al (2015) Energy, economic, and environmental analysis of a flat-plate solar collector operated with SiO2nanofluid. Clean Technologies and Environmental Policy 17:1457–1473. doi: 10.1007/s10098-014-0870-0

Geete A, Dubey A, Sharma A, Dubey A (2019) Exergy Analyses of Fabricated Compound Parabolic Solar Collector with Evacuated Tubes at Different Operating Conditions: Indore (India). Journal of the Institution of Engineers (India) Series C 100:455–460. doi: 10.1007/s40032-018-0455-5

Hazami M, Kooli S, Naili N, Farhat A (2013) Long-term performances prediction of an evacuated tube solar water heating system used for single-family households under typical Nord-African climate (Tunisia). Solar Energy 94:283–298. doi: 10.1016/j.solener.2013.05.020

Jiang L, Widyolar B, Winston R (2015) Characterization of Novel Mid-temperature CPC Solar Thermal Collectors. In: Energy Procedia 70: 65-70. doi.org/10.1016/j.egypro.2015.02.098

Kabeel AE, Abdelgaied M, Elrefay MKM (2020) Thermal performance improvement of the modified evacuated U-tube solar collector using hybrid storage materials and low-cost concentrators. Journal of Energy Storage 29:101394. doi: 10.1016/j.est.2020.101394

Kerme ED, Chafidz A, Agboola OP, et al (2017) Energetic and exergetic analysis of solar-powered lithium bromide-water absorption cooling system. Journal of Cleaner Production 151:60–73. doi:10.1016/j.jclepro.2017.03.060

Ma L, Lu Z, Zhang J, Liang R (2010) Thermal performance analysis of the glass evacuated tube solar collector with U-tube. Building and Environment 45: 1959-67. doi: 10.1016/j.buildenv.2010.01.015

Meyer L, Tsatsaronis G, Buchgeister J, Schebek L (2009) Exergoenvironmental analysis for evaluation of the environmental impact of energy conversion systems. Energy 34:75–89. doi: 10.1016/j.energy.2008.07.018

Mills DR, Bassett IM, Derrick GH (1986) Relative cost-effectiveness of CPC reflector designs suitable for evacuated absorber tube solar collectors. Solar Energy 36:199-206. doi: 10.1016/0038-092X(86)90135-0

Mishra RK, Garg V, Tiwari GN (2017) Energy matrices of U-shaped evacuated tubular collector (ETC) integrated with compound parabolic concentrator (CPC). Solar Energy 153:531-539. doi: 10.1016/j.solener.2017.06.004

Mishra RK, Garg V, Tiwari GN (2015) Thermal modeling and development of characteristic equations of evacuated tubular collector (ETC). Solar Energy 116:165-176. doi: 10.1016/j.solener.2015.04.003

660 Moran MJ, Shapiro HN (1993) Fundamentals of Engineering Thermodynamics, Second Edition. doi:
661 10.1080/03043799308928176

662 Pei G, Li G, Zhou X, et al (2012) Comparative experimental analysis of the thermal performance of evacuated tube
663 solar water heater systems with and without a mini-compound parabolic concentrating (CPC) reflector(C < 1).
664 Energies 5:911–924. doi: 10.3390/en5040911

665 Petela R (2003) Exergy of undiluted thermal radiation. Solar Energy 74:469-488. doi: 10.1016/S0038-
666 092X(03)00226-3

667 Petela R (2005) Exergy analysis of the solar cylindrical-parabolic cooker. Solar Energy 79:221-233. doi:
668 10.1016/j.solener.2004.12.001

669 Rezaie B, Reddy B V., Rosen MA (2015) Exergy analysis of thermal energy storage in a district energy application.
670 Renewable Energy 74:848–854. doi: 10.1016/j.renene.2014.09.014

671 Rosen MA, Dincer I (1997) Sectoral energy and exergy modeling of Turkey. Journal of Energy Resource
672 Technology Transactions of ASME 119:200-204. doi: 10.1115/1.2794990

673 Rosen MA, Dincer I (2003) Exergoeconomic analysis of power plants operating on various fuels. Applied Thermal
674 Engineering 23:643–658. doi: 10.1016/S1359-4311(02)00244-2

675 Saidur R, Ahamed JU, Masjuki HH (2010) Energy, exergy and economic analysis of industrial boilers. Energy
676 Policy 38:2188-2197. doi: 10.1016/j.enpol.2009.11.087

677 Shekarchian M, Zarifi F, Moghavvemi M, et al (2013) Energy, exergy, environmental and economic analysis of
678 industrial fired heaters based on heat recovery and preheating techniques. Energy Conversion and
679 Management 71:51-61 doi: 10.1016/j.enconman.2013.03.008

680 Sokhansefat T, Kasaeian A, Rahmani K, et al (2018) Thermoeconomic and environmental analysis of solar flat plate
681 and evacuated tube collectors in cold climatic conditions. Renewable Energy 115:501–508. doi:
682 10.1016/j.renene.2017.08.057

683 Tsatsaronis G, Morosuk T (2012) Understanding and improving energy conversion systems with the aid of exergy-
684 based methods. International Journal of Exergy 11:518–542. doi: 10.1504/IJEX.2012.050261

685